SYNTHESIS AND CHARACTERIZATIONS OF VISIBLE LIGHT-DRIVEN PHYTO-ASSISTED GOLD NANOPARTICLES BY GREEN CHEMISTRY

Rima ASFARI

FEBRUARY 2022

SYNTHESIS AND CHARACTERIZATIONS OF VISIBLE LIGHT-DRIVEN PHYTO-ASSISTED GOLD NANOPARTICLES BY GREEN CHEMISTRY

A THESIS SUBMITTED TO THE

GRADUATE SCHOOL

OF

BAHÇEŞEHİR UNIVERSITY

BY

RIMA ASFARI

IN PARTIAL FULFILLMENT OF THE

REQUIREMENTS FOR THE DEGREE OF

MASTER OF BIOENGINEERING

IN THE DEPARTMENT OF NATURAL AND APPLIED SCIENCES

FEBRUARY 2022

T.C.

BAHCESEHIR UNIVERSITY

GRADUATE SCHOOL

08/02/2022

MASTER THESIS APPROVAL FORM

Program Name:	BIOENGINEERING (ENGLISH, THESIS)
Student's Name and Surname:	RIMA ASFARI
Name Of The Thesis:	SYNTHESIS AND CHARACTERIZATIONS OF VISIBLE LIGHT-DRIVEN PHYTO-ASSISTED GOLD NANOPARTICLES BY GREEN CHEMISTRY
Thesis Defense Date:	31/01/2022

This thesis has been approved by the Graduate School which has fulfilled the necessary conditions as Master thesis.

Prof. Dr. Ahmet ÖNCÜ

Institute Director

This thesis was read by us, quality and content as a Master's thesis has been seen and accepted as sufficient

	Title/Name	**Signature**
Thesis Advisor's	Assoc. Prof. Dr. Ozan Akdogan	
Member's	Assist. Prof. Dr. Nilay Gunduz Akdogan	
Member's	Assist. Prof. Dr. Canan Bagci	

I hereby declare that all information in this document has been obtained and presentedin accordance with academic rules and ethical conduct. I also declare that, as requiredby these rules and conduct, I have fully cited and referenced all material and results that are not original to this work.

Name, Surname : Rima ASFARI

Signature :

ABSTRACT

SYNTHESIS AND CHARACTERIZATIONS OF VISIBLE LIGHT-DRIVEN PHYTO-ASSISTED GOLD NANOPARTICLES BY GREEN CHEMISTRY

Asfari, Rima

Graduate Program in Bioengineering

Thesis Supervisor: Assoc. PROF. DR. Ozan AKDOGAN

December 2021, 70 pages

Research and development in green-synthesized metallic nanoparticles have grown significantly in recent years, owing to their phenomenal physiochemical properties and biological activities. Bio-synthesized gold nanoparticles (Au NPs) are considered as the most widespread types of nanomaterials produced via green chemistry. Since the plant-based synthesis of NPs emerges as a safer option, two plant extracts were used to fabricate biocompatible gold nanoparticles by the biomass of acai berry powder and bay leaves. The summits in XRD pattern validated the crystallinity through the FCC structure of the gold nanoparticles. On account of their characteristic features such as catalytic properties, these synthesized gold NPs have been developed to be bio-synthetic self-propelled nanomotors with enhanced swimming speeds under visible light. The presence of Au NPs in an aqueous solution with various concentrations of H_2O_2 as a fuel liquid allowed their movement in parallel towards the light source. The reason for movement is due to the electrostatic interaction of the electrons present on the surface of the nanoparticles and the hydrogen atoms of the hydrogen peroxide molecules resulted from the catalytic decomposition of hydrogen peroxide (H_2O_2) on Au NPs surface under xenon light. These catalytically powered nanostructures have gained considerable attention in biomedical and environmental applications.

Keywords: Green chemistry, biocompatible, self-propelled nanomotors, catalytically powered nanostructures.

ÖZET

GÖRÜNÜR IŞIK TAHRİKLİ PHYTO DESTEKLİ ALTIN NANOPARTİKLERİN YEŞİL KİMYA İLE SENTEZİ VE KARAKTERİZASYONLARI

Asfari, Rima

Biyomühendislik Yüksek Lisans Programı

Tez Danışmanı: Doç. Dr. Ozan AKDOGAN

Aralık 2021, 70 sayfa

Yeşil sentezlenmiş metalik nanoparçacıklardaki araştırma ve geliştirme, olağanüstü fizyokimyasal özellikleri ve biyolojik aktiviteleri sayesinde son yıllarda önemli ölçüde büyümüştür. Biyo-sentezlenmiş altın nanoparçacıkları (Au NP'ler), yeşil kimya ile üretilen en yaygın nanomalzeme türlerinden biridir. NP'lerin bitki bazlı sentezi daha güvenli bir seçenek olarak ortaya çıktığından, iki bitki özü, acai berry tozu ve defne yaprağı biyokütleleri, ile biyouyumlu altın nanoparçacıkları üretmek için, kullanılmıştır. FCC yapısındaki nanoparçacıkların kristalliği, XRD verisindeki pik noktaları ile doğrulanmıştır. Katalitik özellikler gibi karakteristik özellikleri nedeniyle, bu sentezlenmiş altın nanoparçacıklar, görünür ışık altında gelişmiş yüzme hızlarına sahip biyo-sentetik kendinden tahrikli nanomotorlar olarak geliştirilmiştir. Yakıt sıvısı olarak çeşitli konsantrasyonlarda H_2O_2 içeren sulu bir çözeltide Au nanoparçacıkların varlığı, ışık kaynağına paralel hareket etmelerine imkan verdi. Hareketin nedeni, nanoparçacıklar yüzeyinde bulunan elektronların ve hidrojen peroksit moleküllerinin hidrojen atomlarının, Au nanoparçacık yüzeyinde ksenon ışığı altında hidrojen peroksitin (H_2O_2) katalitik ayrışmasından kaynaklanan elektrostatik etkileşiminden kaynaklanmaktadır. Bu katalitik olarak güçlendirilmiş nano yapılar, biyomedikal ve çevresel uygulamalarda büyük ilgi görmüştür.

Anahtar Kelimeler: Yeşil kimya, biyo uyumluluk, kendinden tahrikli nanomotorlar, katalitik olarak çalışan nano yapılar.

To My Parents

ACKNOWLEDGEMENTS

In the beginning, I would love to initiate my sincere appreciation to my research advisor Assoc. Prof. Dr. Ozan Akdoğan because of his full supervision, mentorship, punctuality, incessant support, and giving me valuable suggestions, very useful comments throughout my thesis work. He is such an energetic and knowledgeable intellectual that he assisted me in conceiving a new concept and designing the work.

The assistance of Mr. Mehmet Can and Mr. Ibrahim Ertugrul, who are staff members of Bahcesheir University, is considered a corner-stone for the process of fulfilling the lacking parts of my experiments and delivering well-structured feedback related to all aspects of the research.

Away from the research field, my gratitude and love are sent to my friends and colleagues, both inside and outside of the university, for their unwavering support during this period. A heartful applaud goes to Mayan Massarani, Haydar Ayad, Lyne Badaoui, and Yazan Odeh.

Above all, this is the right time to present my deepest gratitude to my family for all the things they have done in my life, who I cannot repay their kindness towards me.

This work was supported by BAP. 2021.01.17 (Bahcesehir University).

Istanbul, 2021 Rima Asfari

TABLE OF CONTENTS

TABLE OF FIGURES

FORMULAS

ABBREVIATIONS

VIS	Visible Light.
UV	Ultraviolet.
SPR	Surface Plasmon Resonance.
LSPR	Localized Surface Plasmon Resonance.
FCC	Face-centered Cubic.
XRD	X-Ray Diffraction.
TEM	Transmission Electron Microscopy
ICP	Inductively Coupled Plasma Spectrometry.
AB	Acai Berry.
BL	Bay Leaves.
CAD	Computer Aided Drafting.

Chapter 1
Introduction

Nanotechnology is a recent scientific breakthrough that is evolving at a very fast pace. Many related industries have grown rapidly in recent years with the advent of nanotechnology. In general, metal nanoparticle production is made possible through two protocols, which are top-down and bottom-up processes. Most of the techniques involve high temperatures, vacuum conditions, and toxic chemicals. As a result, side effects could affect organisms including humans (Balasooriya et al., 2017).

The creation of metal NPs have been implemented by conducting different chemical and physical techniques, as an illustration; heat evaporation, photochemical reduction and chemical reduction. (Dubey, Lahtinen, & Sillanpää, 2010). However, the advances in green chemistry field in the generation of MNPs has offered secure and cost-effective approaches based on plant extracts in recent years. Plant extracts produce more stable nanoparticles, and the formation rate is quicker and simpler than other methods. (Hamelian, Hemmati, Varmira, & Veisi, 2018). The reduction of metallic ions into Nanoparticles is caused by the biomolecules which are derived from the extract of the plants (KSV, 2017).

Metal nanoparticles (MNPS) have attracted enormous attention due to their scientific and technological significance, as well as they have distinct electronic, chemical, optical, and magnetic capacity that vary significantly than those of single atoms and their mass counterparts. (Gericke & Pinches, 2006) Gold nanoparticles (GNPs) are widely used in implications., which include medical applications; biosensing (Phiri et al., 2019), cancer detection, especially gold nanoparticles with specific antibodies provides a promising probe for the specific identification of cancer cells (Cho et al., 2017). Furthermore, gold nanomaterials have been widely employed as vaccination platforms due to their various shapes, sizes, and customizable surface properties like virus testing and detection by adding specific biomolecules to their surfaces (Draz & Shafiee, 2018). They also exhibit excellent catalytic performance, for instance, they can degrade organic dyes pollutants into non-toxic products (Garg et al., 2020). In the field of agriculture, gold NPs-based sensors could be employed to evaluate the herbicides in plants and food items, for instance, the use of gold

nanoparticles that obtained from bacteria to identify residue levels of organic compounds in vegetables and crops has been demonstrated (Malarkodi et al., 2017).

The interest in Au nanomaterials arises from the simplicity of production, which allows for precise control over their morphologies and sizes. All preparation methods of Au nanomaterials rely on the reduction of gold ions, and for this purpose, the most used salt is $HAuCl_4$ (Zeiri et al., 2014). In this study, different sizes of gold nanoparticles were produced utilizing two plant extracts to reduce and stabilize the NPs. One extract was obtained from acai tree's fruit, *Euterpe oleracea Mart*, a palm tree attributed to the Amazon region, while the other was made from *Laurus nobilis* leaves known as Bay leaves (BL). However, these differently synthesized gold nanostructures were only measured on the basis of their sizes.; an average of (28 ± 5) and (20 ± 2) nm of size distribution and spherical gold nanoparticles are resulted from both extracts; acai berry-Au nanoparticles and bay leaves-Au nanoparticles, respectively. Nonetheless, because research on biosynthesized acai berry-Au NPs still is limited, we largely focused on them.

The sizes of acai berry-Au nanoparticles were monitored through changing the quantity of these extracts in the reaction medium. The gold nanoparticles obtained were distinguished by UV/vis spectroscopy, Fourier Transform Infrared Spectroscopy (FTIR), transmission electron microscopy (TEM), X-ray diffraction (XRD), and inductively coupled plasma spectrometry (ICP). The spherical shape of fabricated Au NPs were observed by the size of 16 nm, which was the dominant shape in TEM images.

The present study also aimed to extend the research by making these photoactive gold nanostructures steerable with enhanced swimming speeds when they are exposed to light with constant-intensity (VIS) light in the medium contains H_2O_2. This study aimed to green synthesize gold nanoparticles and screen their ability to exhibit their propulsion and control them depending on the direction of incoming light.

Chapter 2
Literature Review

2.1 Nanoparticles

Nanoparticles are materials that have properties that vary from their bulk and molecular equivalents., and they are the building blocks for nanotechnology (Biswas & Wu, 2005). Nano is a word that is originated from the Greek word that means "dwarf", it is a term to characterize any substance that has components less than one hundred nanometer in at least one dimension. Nanoparticles are types of structures with a diameter range between 1 to 100 nanometers (Batacharyya et al., 1995). Nanoparticles have the potential to be fabricated in several morphologies and sizes (Kowalczyk et al., 2011). The highly interest of nanoparticles regarding their tiny size and high surface-to-volume ratio, that causes chemical and physical variations for their properties. This phenomenon can increase their reactivity, as well as their ability to infiltrate cell membranes and potentially perform a bio-chemical activity (Dubchak et al., 2010). In the UV–Visible region, metallic nanoparticles can absorb light at their (SPR) surface plasmon resonance. Because of the small particle size, the surface plasmon band results from the coherent presence of unpaired electrons on the NP's surface in the conduction band (Sharma et al., 2009). Recently, researchers are spotting a light on the synthesizing of nanoparticles by green chemistry administrating noble metals such as silver (Ag), gold (Au), zinc (Zn), platinum (Pt), and palladium (Pd) owing to their uses in therapeutic and pharmaceutical fields, as well as their usage in consumer stuff such as soaps, hair products, cleaning products, and cosmetic materials (Vijayakumar et al., 2016).

2.2 Gold Nanoparticles

Gold holds a unique position among the metals in the periodic table of the chemical elements. It is the most noble of the metals. Its inert nature prevents

interaction with components of the atmosphere demonstrating its lack of reactivity. Due to its resistance towards most corrosive forces, it has been known as “King of the Metals”. For example, gold historical artifacts can keep their bright sparkle for thousands of years without corrosion for example, chemical oxidation, or damage (Schmidbaur et al., 2005). What makes gold so attractive are the color and the luster of this metal. Gold is a noble element that derived its color from yellow, it can also be found purple, ruby, or black when ultra-milled in certain conditions. Some of gold’s characteristics are malleability and ductility, meaning it can be pounded into different shapes and stretched into a wire (Laguna, 2008).

The interest of scientists has been increasing since they discovered that gold is divided into tiny pieces, for instance, gold nanoparticles. In the past thirty years, there has been a surge in this scientific enthusiasm in a variety of fields. Gold, for example, was previously thought to be chemically inactive. The huge discover in 1987 emphasized on the fact that gold nanoparticles have great catalysts when they are do not exceed 5 nanometers. (Louis & Pluchery, 2017). Furthermore, gold possesses the smallest electrochemical ability of any other metal, which means that any cationic phase of gold has the ability to gain electrons from any donors, such like reducing agent, to produce Au metal. In other words, it is the metal with the greatest electronegative potential of any metal. (Laguna, 2008).

Researchers are interested in gold nanoparticles (Au NPs) because of their wide variety of applications in areas including biomedical applications (Cai, 2008). Additionally, gold nanoparticles have been carried out in protein assay (Tang et al., 2007), screening of cancer cells (Medley et al., 2008), as well as immunoassay (Liu et al., 2008).

2.2.1 General characteristics of gold nanoparticles (Au NPs). The distinctive chemical and physical characteristics of Au metal are responsible for its widespread applications at both the macroscopic state and the nanoparticulate state. The metallic radius of gold (0.14420 nm) is smaller than that of silver and copper, and it crystallizes into a face-centered cubic (FCC) structure (figure 1). This structure allows it to be malleable; a surface area of about 1 meter of a gold foil can be obtained under the process of battering. Moreover, a 165 m golden wire of 20 μm in size can be articulated from the same amount of gold in the previous example which is 1 g. (Louis & Pluchery, 2012).

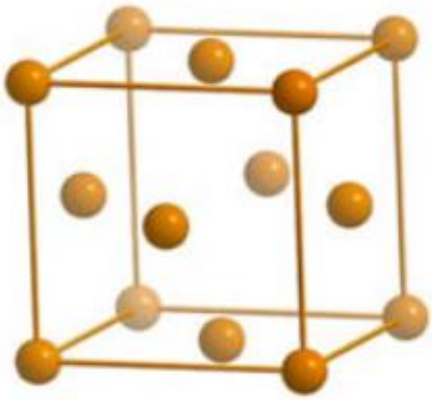

Figure 1. FCC gold structure (Zeng & Jin, 2014).

2.2.1.1 Biocompatibility. Biocompatibility is defined as a material's ability to perform its intended functions concerning medical therapy, to elicit a proper host engage in a particular implication, and to have interaction with a living organism that does not lead to any injury, poisonous, or immune system is refusing it. (Ghasemi-Mobarakeh et al., 2019). A fundamental case in assessing the biocompatibility of nanoparticles is estimating their possible cytotoxicity, because of their shape, size, properties, chemical composition, or because of the interaction of the nanoparticle surface with the cells (Shukla et al., 2005). Despite the fact that Au nanoparticles are biocompatible, in some situations; gold nps with deposited chemical substances on it could create a negative impact in certain therapeutic applications. However, the use of biosystems or plants in the nano particles generation has the capacity to overcome this critical issue by manufacturing more biocompatible nps. (Smitha et al., 2009). The possible advantages of nanomaterials in biological and manufacturing implications are enormous, little is known about their possible short- and long-term deleterious impacts on human and environmental health (Connor et al., 2005). A great attraction has been created towards the nanoparticles by the medical field representatives in cancer detection studies, therapy, in addition to transporting vectors for both, biological and pharmacological drugs. For a variety of reasons, gold nanoparticles (GNPs) are particularly intriguing. First, they are easily prepared. Furthermore, Compounds like pharmacologic agents, carbohydrates, and antibodies can easily be bound to GNPs and identify cancer cells. Additionally, the GNPs themselves have anti-angiogenic properties (Gannon et al., 2008).

2.2.1.2 Chemical stability. Gold is chemically inert and can resist corrosion. These remarkable physical properties of the gold make it biocompatible for medicinal purposes; it is ideal for medical use, including skin cancer, syphilis, ulcers, smallpox, measles, and AIDS (Ananda Chitra, 2016). It should be mentioned that other metals that may have similar properties to gold are platinum and silver, but platinum is more costly than gold and silver is highly reactive (Safavi et al., 2008). Because of their considerable chemical stability, gold nanoparticles have significant roles in the medical treatment field, making preparation and manufacturing techniques simple, straightforward, and less harmful (Yaqoob et al., 2020).

2.2.1.3 Localized surface plasmon resonance. When discussing plasmon resonance, two distinct concepts are referred to as plasmon resonances. When an impulsive wave hit the metallic surface, this is came to as surface plasmon resonance. (Louis & Pluchery, 2012), while the excitation of unpaired electrons in the conduction band at the surface of metallic nano-objects resulting from interactions with photonic wavelengths is referred to localized surface plasmon resonance (LSPR). (Link & El-Sayed, 2000). It is described as a small part of the main spectral characteristics of LSPR is when the plasmon resonance presents in the visible or near-infrared range for Au or Ag NPs. This effect occurs when an incident light passing throughout a homogeneous nanoparticle assembly is partly absorbed in the plasmon resonance frequency, resulting in an optical spectrum with a dramatic absorption at ɷ plasmon (which corresponds to the LSPR peak) (Louis & Pluchery, 2012). Furthermore, the environment near the particle surface has a big impact on the LSPR. When the molecules that are absorbed on the NP surface change, for example, the LSPR shifts. (Louis & Pluchery, 2012).

At about 520 nanometers in the spectrum, the intense red color of Au nanomaterials solutions in water and glasses exhibits this phenomenon. (Daniel & Astruc, 2004). This feature is the physical origin of the strong light absorption by noble metals (El-Brolossy et al., 2008). Some intrinsic or extrinsic parameters influence the LSPR's characteristics by shifting the band of the plasmon resonance: the adjacent medium of the particles, the morphology of the nanoparticles, and using core-shell nanoparticles. In the case of spherical particles, the LSPR's intensity is affected by the

sphere's volume. However, the diameter of the particles does not have influence on the LSPR band placement (Louis & Pluchery, 2012).

Moreover, metal nanostructures such as silver and gold nanoparticles show the shape-dependent SPR in the visible range (Zhuang et al., 2018). Owing to their intense surface plasmon resonance, the widely used nano structural substances in molecular imaging and biomedical therapeutics are the Au NPs. (Balasubramanian et al., 2010).

2.2.2 Heterogeneous catalysis. The photocatalyst in heterogeneous photocatalysis is commonly a semiconductor metal which has the capability of receiving incoming photons. In this effect, photocatalytic reactions, such as the oxidation of donors and the reduction of electron acceptors take place either at the semiconductor's linkage with the gaseous or liquid medium (typically aqueous) or in the liquid surrounding it (Zhang et al., 2009). The strong coupling of light with metal nanoparticles at specific photon energies is caused by the optical excitation of the metal's collective electronic resonances, known as surface plasmons.

The fundamental principle of photocatalysis is the formation of electron-hole pairs upon light absorption. Creating the electron-hole pairs on the metal surface, causing reduction and oxidization of two corresponding entities that are present in the medium. The hole that was created by the photons in the valence band (h^+vb) and the excited electrons in the conduction band (e^-cb) are the oxidative and reductive species. (Curti et al., 2016). Catalytically induced nanoscales are driven because of the biodegradation of a specific liquid on the upper layer of the catalyst hence, creating ahead movement (Wang et al., 2015). As an illustration, the photocatalytic induced reaction of water splitting is illustrated in figure 2 (Mateo et al., 2016).

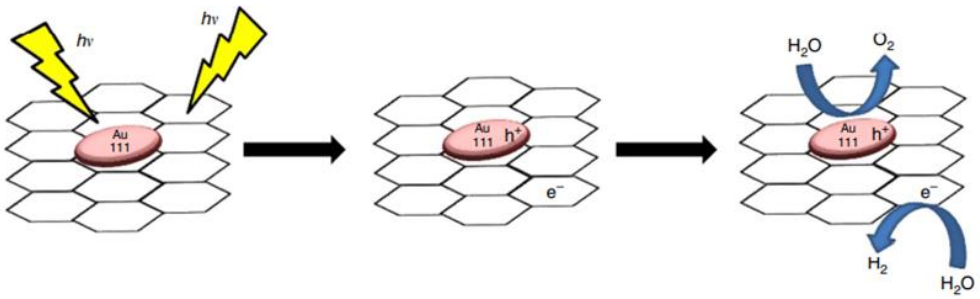

Figure 2. Photocatalytic induced decomposition reaction (Mateo et al., 2016).

External fields, particularly electric (Loget & Kuhn, 2011) and magnetic fields (Dreyfus et al., 2005), have been used to propel motors at the nano and micro scale.

Due to this phenomenon, self-propelled-nanoscaled devices have emerged and drawn considerable attention because of their potential applications in environmental remediation (Orozco et al., 2013), cargo transportation (Patra et al., 2013), biomedical applications (e.g., targeted drug (Ceylan et al., 2017) and gene delivery (Duan et al., 2015).

2.3 Types of Gold Nanoparticles

Gold nanostructures can be divided into several subtypes depending on their size, shape, and physical traits.

- Gold nanospheres
- Gold nanorods
- Gold nanoshells
- Gold nanocages

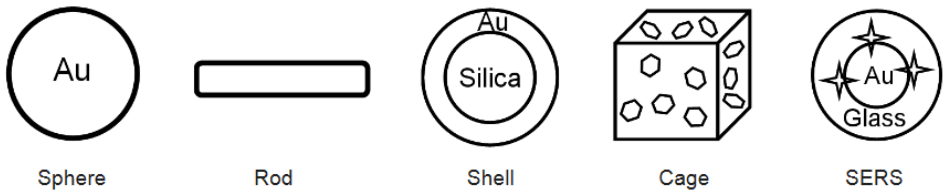

Figure 3. Different types of gold nanoparticles (Cai, 2008).

Gold nanospheres: also known as gold colloids, with diameters ranging from 2 nm to over 100 nm. they can be synthesized by reducing an aqueous $HAuCl_4$ solution with different reducing agents under various conditions. By changing the reducing agent/gold ratio, the size of nanospheres can be controlled. They have a single absorption peak in the visible range between 510 and 550 nm. The absorption peak shifts to a longer wavelength as particle size increases, and the width of the absorption spectra is proportional to the size distribution range (Turkevich et al., 1951).

Gold nanorods: the commonly used methodology to produce gold-rod shaped nanoparticles is relying on the decomposition of the metal gold inside the pores of nanoporous poly carbonate or alumina template lyres. Due to the cylindrical form of the membrane pores, a nanocylinder of the desired substance is obtained in each pore (Martin, 1996). Gold nanorods (AuNRs) have received the most attention of all the anisotropic (nonspherical) MNPs (Lohse & Murphy, 2013).

Gold nanoshells: These structures have a strong surface plasmon resonance in the near-infrared (NIR) spectrum. These Au nanocomposites benefit *in situ* cancer therapy as they can be excited by NIR radiation, which invades tissue more strongly than shorter wavelength irradiation. The inner core of gold nanoshells is composed of silica, while the external layer is gold. The thickness of the shell is controlled by gold (Chu & Wu, 2011).

Gold nanocage: gold nanocages are unique types of nanomaterial that has porous walls and hollow interiors. They're produced with a relatively simple galvanic replacement reaction between Ag nanostructures formed through polyol reduction and metal precursor salt solutions (Au) formed through polyol reduction. (Qiu et al., 2020). When the electrochemical capability of the two types differ and the reduced metal is

accumulated on the Ag surface, the reaction is triggered. Changing the amount of metal precursor added to the suspension of Ag nanocubes has been discovered to be a simple way of tuning both the composition and the localized surface plasmon resonance (LSPR) of the metal nanocages. Many structures for biomedical and catalytic applications have been developed using this method (Skrabalak et al., 2008).

2.4 Synthesis of Gold Nanoparticles

Generally, Au NPs are produced when gold ions are reduced using reducing agent, for instance, borohydride, citrate, hydrazine, and others, accompanied by surface modification with an appropriate capping agent to avoid the particles from aggregation by binding to the newly formed particle's surface providing stability, modifying surface reactivity. This allows for more control over nanoparticle size and polydispersity (Dahl et al., 2007). This methodology includes the assembly of atoms (generated by ions reducing) into desired nanostructure, which is called the Bottom-Up approach (Herizchi et al., 2014). While the Top-Down process is the removal of molecular and atomic particles from an originally big-sized material to elaborate the desired nanoparticle (KSV, 2017).

However, many conventional approaches, such as chemical and physical proccesses, have been used effectively to form several inorganic nanomaterials, but they are expensive and involve the usage of hazardous chemical substances. As a result, our environment is being severely harmed, and many harmful compounds are being released (Kanchi & Ahmed, 2018). Besides, these traditional procedures often yield polydisperse nanoparticle populations, necessitating extra separation processes to generate monodisperse populations (Murphy, 2002).

2.4.1 Green synthesis. Many recent studies have shown that living organisms such like algae, fungi, yeast, bacteria, and human cells, as well as plants, have the ability to serve as a possible source for the production of nanostructures in healthy processes. These organisms are rich in proteins and metabolites therefore, inducing dicrease of the metal salt solutions to convert it into metallic NPs. Bio-organism-based synthesis is compatible with green chemistry principles (Parveen et al., 2016).

In the past numerous years, traditional methods are used, but according to studies, green approaches are efficient enough to yield a great amount of metal NPs with lesser errors rates, lower costs, and simplicity of identification. Moreover, they are preferred over conventionally delivered NPs because adding more chemicals that are hazardous and harmful to human well-being and the environment may increase the reactivity and toxicity of the particle, as well as produce unintended negative health effects. (Gour & Jain, 2019). It's worth noting that the reducing agent, capping agent, and reaction medium are all crucial components in the fabrication and stabilization of metal NPs; these issues should be addressed extensively from a "green chemistry" and economic viewpoint. Most of the synthetic processes published on this topic depend primarily on organic solvents (mostly due to the hydrophobicity of the CA used), eventually leading to serious ecological issues while dealing with industrial production. Yet, several capping agents, such like oleic acid and thiols, have been extensively used in generation of magnetic and metal nanoparticles in organic solvents. (Brust et al., 1994).

2.4.1.1 Plant mediated gold nanoparticles production. Plant-based nanoparticle synthesis is a green chemistry approach connecting plant biotechnology to nanotechnology by creating genetically modified plants that are pesticide and herbicide-resistant, providing the desired chemicals in high quantities and facilitating their isolation to be used in nanoparticle synthesis (Parveen et al., 2016; Kalia, 2018). The biogenic decrease of metal elements using plant extracts has become one of the most widely acknowledged systems for manufacturing NPs because it is regarded as an environmentally friendly and cost-effective technique that does not require the use of chemical pollutants (Hernandez-Diaz et al., 2020). Moreover, plants are abundant in nature, easy to get when needed thus, plant extracts are more ideal compared to

microorganisms for the generation of metallic NPs at large scales (Iravani, 2011) The bio-fabrication of nanoparticles represents a bottom-up approach in which the primary reaction is reduction/oxidation (Naik et al., 2002). A plant extract assisted bio-reduction typically requires combining the green extract solution with a metal precursor solution of the relevant metal. The reaction happens at the ambient temperature and is usually finished in a short time (Mittal et al., 2013).

Reducing and stabilizing agents, and solvent medium are all necessary constituents for the biogenesis ofmetallic NPs. Plant extracts are considered to be reducers and stabilizers at the same time. An extract's bio-reducing and stabilizing potential is most likely related to its natural products, which includes phenolics, flavonoids, vitamins, phenolic acid, glycosides, terpenoids, organic acids, polysaccharides, and proteins (Nasrollahzadeh et al., 2019). Each plant has its own concentration of these active components, and this concentration differ from one plant to another. Mixing metal precursors with components coming from different plants will elaborate distinct nanoparticles (triangles, pentagons…etc.) (Kanchi & Ahmed, 2018). Many scientists have displayed the capability to produce gold nanoparticles from a variety of plant extracts. The first one was reported by (Gardea-Torresdey et al., 2002). Furthermore, Au NPs were formed in live alfalfa plants (*Medicago sativa*).

2.5 Factors Influencing Gold Nanoparticles Synthesis

After choosing the ideal plant extract and in order to acquire appropriate nanoparticle properties, metal precursor, green extract volume, temperature, response time, and pH must be ideally analyzed (Lee et al., 2020).

2.5.1 Impact of metal ion concentration. There is a crucial element that determine the morphology, size and reaction time in the process of nanoparticles synthesis which is the metal ion concentration. Au NPs were synthesized through combining various amounts of tansy fruit extract. An important correlation exists between the particles size, absorbance peak, and the concentration of ion metal. However, it was shown that the increase in the concentration of metal ion have caused an augmentation in particles size and absorbance peak. In contrast, it was demonstrated that when the metal ion

concentration was reduced, the particle size, synthesis rate, and absorbance peak were all diminished. Moreover, there was shrinking in particle size, synthesis rate and the peak of absorbance when the concentration of metal ions was low (Dubey et al., 2010).

2.5.2 Plant extract concentration influence. Adjusting the plant extract concentration control the rate of reaction and dimensions of nanoparticles. However, previous studies have shown that a rise in absorption peaks and a reduction in the gold nano-colloids size of the particles occurred in parallel to an increase in the plant extract ratio. This phenomenon was based on the UV-VIS spectra (Dwivedi & Gopal, 2010).

2.5.3 pH influence. Research shows that pH values can vary remarkably in extracts collected from a single plant depending on the part it was harvested from. For that reason, the optimization process was found to be crucial in synthesizing NPs. In one study, it was revealed that the higher pH values contribute to producing Au NPs reduced in size due to shorter wavelengths in the SPR band (Armendariz et al., 2004) (Choudhary et al., 2020) (Costa et al., 2020).

2.5.4 Temperature influence. Another element that may influence the development of Au-NP synthesis is temperature. The synthesis of bimetallic Au-Ag NPs in a comparative study involved the reduction of the ions of Au and Ag by the extract of Anacardium occidentale leaf from low to high temperatures to obtain the appropriate result. For steady NP generation at lower temperatures, more extract was required. (Sheny et al., 2011)

2.5.5 Influence of incubation time. The synthesis duration has a significant impact on the yield size, shape, stability, and optimal NP synthesis. In 2017, Eskandari-nojedehi et al. synthesized AuNPs from mushroom extract (Agaricus bisporus). It was discovered that raising the NPs synthesis time improve the development rate of the Au-NPs, which in turn reducing the particle size.

2.6 *E. oleracea* (Acai Berry)

2.6.1 Botanical description. Acai palm, referred as Euterpe oleracea Martius, is a tiny purple-black colored (indigo) berry grown in South America, and is mainly found in different countries including Brazil and Suriname. It was also discovered that this palm tree can be harvested from Amazonian areas. This plant, shown in figure 4, measures approximately 10 to 12 mm when it is fully matured (Schauss et al., 2006; Gallori et al., 2004).

Figure 4. Acai (*Euterpe oleracea*) palm trees (lift). Hundreds of mature acai (*Euterpe oleracea*) fruits (right). (De Oliveira & Schwartz, 2018).

2.6.2 Bioactive compounds. Acai berries are composed of phenolic chemicals offering a promising source of antioxidants blocking the incidence of many cardiovascular and brain diseases. Healthy participants who consumed Açai pulp and juice showed a rise in antioxidant concentration in blood (Mertens-Talcott et al., 2008). Antioxidants are natural substances that get rid of free radicals and considered toxic to human bodies where they can disrupt major cellular entities incorporating into carbohydrates and nucleic acids. However, these substances are synthesized naturally in the absence of oxygen (Hangun-Balkir & McKenney, 2012). Being rich in flavonoids (31%), lignoids (11%), proteins (6% to 12%), lipids (21% to 53%), phenolic compounds (23%), in addition to fibers (17% to 71%), anthocyanins (9%) and carbohydrates (36% to 43%) makes this specie a "superfruit" (Freitas et al., 2021).

2.7 *Laurus nobilis* (Bay Leaves)

2.7.1 Botanical description. Laurus nobilis L. (Lauraceae family), also known as bay, is considered one of the ancient herps and is highly utilized as a seasoning. This tree (figure 5), consisting of approximately 30 genera and 2.000 to 2,500 species, is grown in the Mediterranean areas. However, it is known as Apollo's Laurel in mythology and is widely cultivated as a flowering plant in European countries and in the U.S (BARLA et al., 2007). The leaves and fruits of L. nobilis are utilized in medicine care all over the world, in addition to its important status as a culinary herb. Laurel oil or butter, derived from the fruits (berries) of L. nobilis, is an important component of laurin ointment, a popular treatment for rheumatism, gout, and spleen and liver diseases. It can also be used in veterinary medicine. (Sharma et al., 2012)

Figure 5. The leaves of *Laurus nobilis* plant (Bay leaves) (Patrakar et al., 2012).

2.7.2 Bioactive compounds. Laurus nobilis is primarily found in countries near the Mediterranean Sea and is rendered as a provider for abundant quantities of polyphenols. Phytochemical studies demonstrate that bey leaves are basically composed of 1,8-cineole, linalool, and α-terpinyl acetate. Furthermore, the most abundant phenolic compounds are procyanidin dimers and trimer, in addition to epicatechin, flavonol, and flavone derivatives. Bay leaves contain specific bioactive compounds utilized in seasonings and preservatives in several products such as pharmaceuticals, fragrances, and cosmetics. Consequently, this plant's extracts are considered valuable and profitable (De Matteis et al., 2021; Boulila et al., 2015; Dias et al., 2014; Ertas¸and Alma, 2010; Ertas¸and Alma, 2010).

Chapter 3
Materials and Methods

3.1 Chemicals

Euterpe oleracea powder was bought from the vegan market, Istanbul, Turkey. Hydrochloroauric acid ($HAuCl_4$) powder (Sigma Aldrich, St. Louis, Missouri, United States), hydrogen peroxide (H_2O_2) (%35, Inter lab), ethanol (99.9%, Iso Lab).

3.2 Green Synthesis of Gold Nanoparticles

3.2.1 *E.oleracea* (acai berry)

3.2.1.1 Extract preparation. Before the preparation of gold nanoparticles, the stock solution of 10% Açai berry (AB) was prepared in double-distilled water. 3 g of its finely ground powder was taken in a beaker containing 30 ml of double distilled water to make it 10%, then boiling the mixture on a magnetic stirrer for 1 hour at 76 °C. After that, the extract was filtered using filter paper.

3.2.1.2 Gold nanoparticles biosynthesis. To a vigorously stirred 60 ml of 1 mM aqueous HAuCl4 solution, 10 ml of the green extract was added and stirred for 2 hours. The NPs were washed three times with ethanol (99.9%) and then centrifuged at 15000 rpm for 6 min to remove unreacted biomolecules. After that, the nanoparticles were stored at 4ºC for further use. At room temperature, the preparation reaction took place. Gradual reduction of gold ions and the generation of Au NPs could be seen visually as the reaction mixture's color changed to deep violet as evident from figure 6. All obtained gold nanoparticles were purified by four ethanol washing/centrifugation steps. For the fabrication of different sizes of Au NPs, the quantity of the reducing agent is varied as 5, 10, and 15 ml.

Figure 6. The deep violet color of synthesized gold nanoparticles.

3.2.2 *Laurus nobilis* (bay leaves)

3.2.2.1 Extract preparation. Healthy bay laurel leaves purchased were purchased from the local market in Istanbul, Turkey. Before use, the leaves were washed several times with deionized water to remove any dust. Then, they dried in the shade and the plant material was ground with a coffee blender to obtain a powder and sifted through a 0.5 mm mesh screen to achieve a uniform particle size. In a 200 ml Erlenmeyer flask, approximately 24 g of the leaf powder was added to 120 ml of distilled water to make 20% (v/v) of stock solution (figure 7). The mixture boiled on a magnetic stirrer for one hour at 76 °C. After that, the extract was filtered using filter paper and cooled to room temperature. The filtrate was collected and stored at 4ºC for further use.

Figure 7. Bay laurel leaves extract.

3.2.2.2 Gold nanoparticles biosynthesis. 60 mL aqueous solution of 1 mM of auric acid (HAuCl4) was reduced using 10 mL of bay leaves extract at room temperature for 2 hours, resulting in a pink-red solution indicating the formation of gold (AuNPs) as shown in figure 10. The NPs were washed three times with ethanol (99.9%) and then centrifuged at 15000 rpm for 6 min to remove unreacted biomolecules. As the reaction mixture's color changed from brown- yellow to reddish blue, the reduction of gold ions and generation of Au NPs could be seen visually as shown in figure 8.

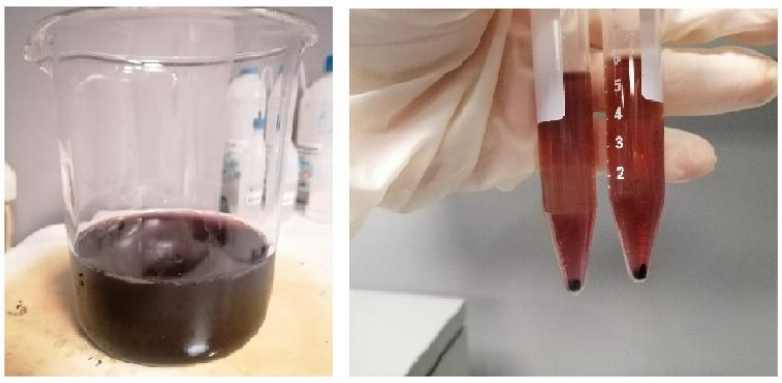

Figure 8. The deep pink-red solution indicated the formation of gold nanoparticles from bay leaves.

3.3 Issues with Source of Light and Fabrication Type of Nanomaterial

Firstly, we employed a halogen bulb (figure 9) in our first trial as a source of light in an open system. The bulb radiated a spectrum of mostly visible light with a slight closeness to infrared radiation in the interval between 480 to 1000 nm (figure 10). The problem was the intense emitted brightness resulting in a great deal of heat. Besides, the high power of the bulb has led to a rise in the temperature of the whole setup, causing the creation of undesired bubbles on the surface of the fuel solvent and the walls of the container. To resolve this issue, we created a dark closed system with the same environment but with a different light source, which was previously mentioned as the xenon lamp. This lamp was much cooler than the latter because it uses less energy due to the ballast which helps regulate the electric current.

Figure 9. The halogen bulb.

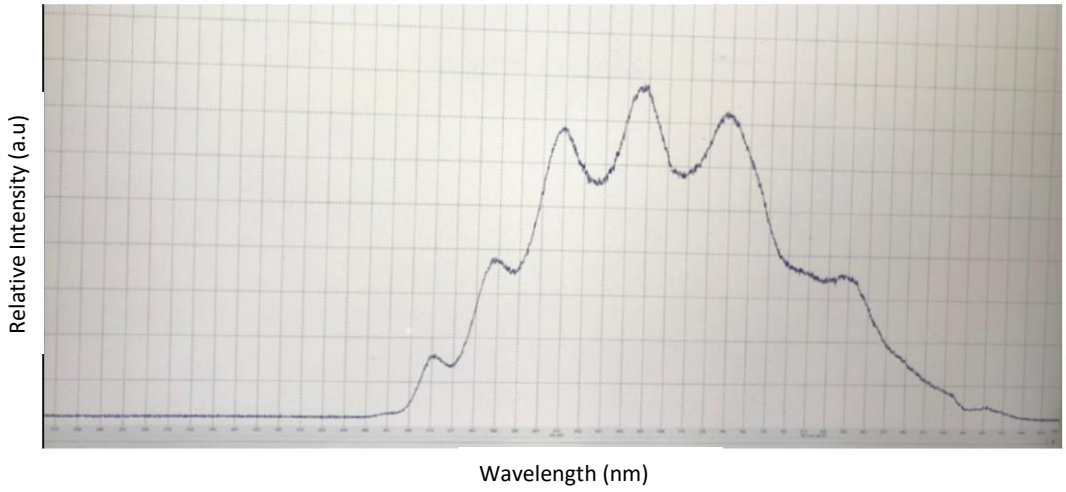

Figure 10. The spectrum of a halogen bulb.

Another issue is the usage of additive materials such as hydrogel and resin-based gold nano/microswimmers to make them float in the solvent. Regarding the pre-synthesized acai berry-Au nanoparticles and the swimmers, they were tried with halogen light, but the halogen bulb was not suitable to induce the chemical reaction on the metal surface to make them move. Nonetheless, the light intensity participates in raising the temperature remarkably even in a few minutes, forming bubbles in the solution.

The significance of our study is to present that the temperature does not affect propulsion. To overcome this challenge, we believed that the xenon lamp will be an appropriate alternative to self-propelled nanostructures. Starting from this point ahead, we could modify the experimental design by changing the source light and conducting it in a closed system. In this case, only a slight increase in the temperature during xenon illumination was observed, which is far smaller than the increased rate observed under halogen illumination. This method was effective in making the biosynthesized Au NPs self-propelled. However, when it came to the use of gold swimmers, they would dip to the bottom of the experiment medium without any noticeable movement. The same failed result was obtained when the illuminance of the xenon was applied to the resin-based gold microswimmers.

3.4 Light Setup

The setup used to actuate the movement of gold nanoparticles consists of an 85 V xenon bulb. It is a type of gas discharge lamp that produces a bright white light (brightness intensity of 35 W) when electricity passes through ionized xenon gas. The Xenon lamp used in this experiment emits a broad visible spectrum in the 400-700 nm wavelength range as could be seen in figure12. Ballast, power supply, and two powering cables are also main constituents of the light system as illustrated in figure 11. The ballast is an essential part of a fluorescent lighting system that supplies the voltage required to start the lamp and regulates the electrical current of the light once it is lit. One of the cables is connected to the power supply to provide power to the ballast, and the other one is used to connect the output of the ballast to the xenon lamp.

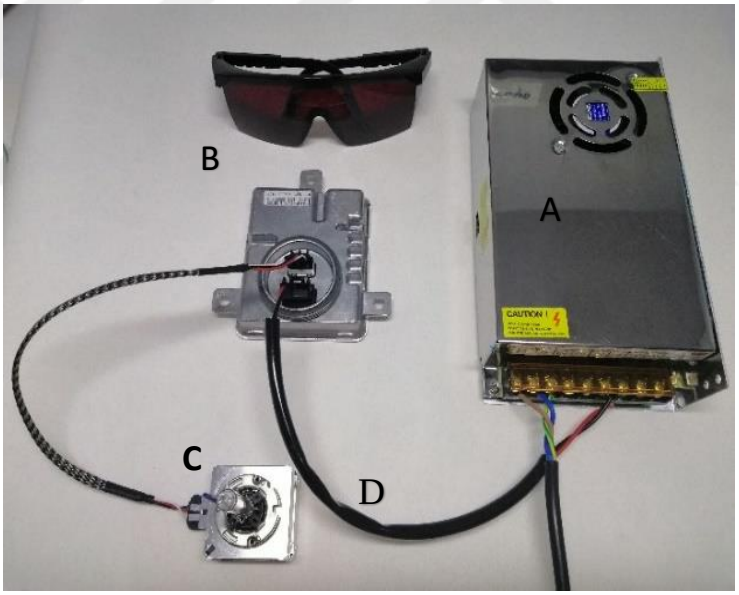

Figure 11. HID light setup components: (A)power supply. (B) the ballast. (C) the xenon lamp. (D) powering cables.

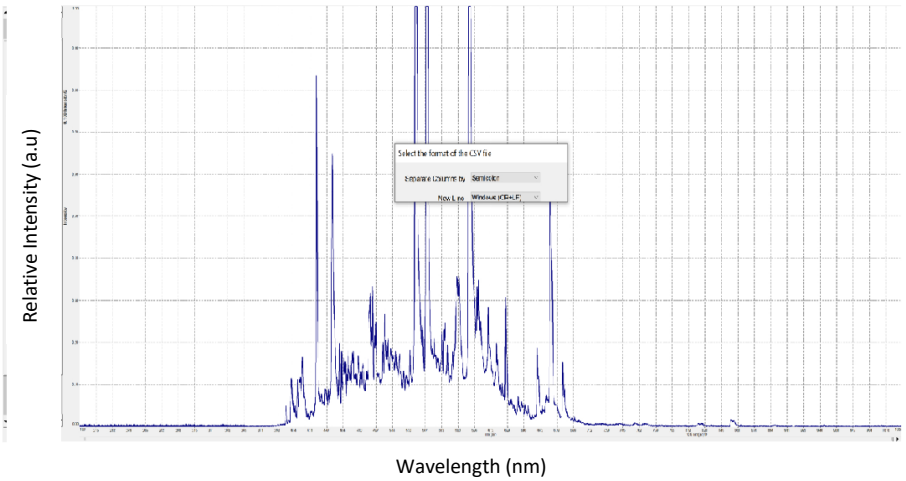

Figure 12. The UV-vis spectrum of a xenon bulb.

3.4.1 Controlling the self-movement of gold nanoparticles by VIS light in a dark system. The gold nanoparticles were suspended in three different concentrations of H2O2 (2%, 4%, and 6%) in a small plastic container that can hold ≈16 ml of liquid. This container then was placed in a closed dark system provided with one hole on each side of the system. The xenon lamp was incident on the nanoparticles through the holes of each side. Accordingly, the angle of light projection on these Au NPs exposed to visible light will respond as shown in figure 13. This system was made to investigate the navigation capability of the nanoparticles controlled by an external illuminating source.

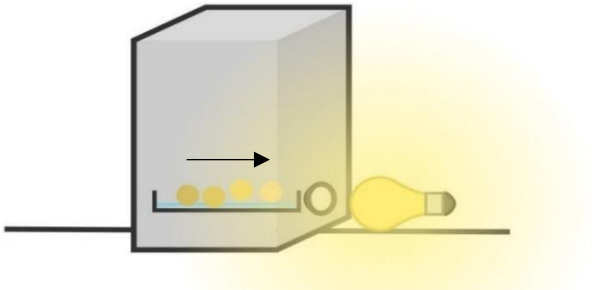

Figure 13. Controlling the self-movement by external VIS light in a dark system.

The gold nanoparticles accelerate in speed while moving towards the light source with increasing the concentration of peroxide fuel at room temperature. The movement of these nanoparticles was recorded with a camera for further analysis and velocity calculations.

3.5 Characterization

UV-vis spectroscopy was used to confirm the LSPR wavelength of gold nanoparticles (Shimadzu UV-visible spectrometer UV mini-1240). JEOL 3010 is a high-resolution transmission electron microscopy (HRTEM) that was used to measure the morphology of the particles. The X-ray diffraction data was taken by using Bruker D2 Phaser. The Perkin-Elmer Spectrum 100 device was used to measure the FTIR data. The gold nanoparticles production yield was determined using Inductively coupled plasma spectrometry (ICP-OES) Perkin-Elmer-Optima 7000 DV.

Chapter 4
Results

4.1 XRD Result

Figures 14 and 15 confirmed the crystalline nature observed for the colloidal gold nanoparticles from the two extracts through X-ray diffraction (XRD) analysis. By using acai berry and bay leaves extracts, four peaks were noticed at 38.21º, 44.31º, 64.71º, 77.81º and 38.1, 44.4, 64.8 and 78 which corresponds to the (1 1 1), (2 0 0), (2 20) and (311), respectively. These intensities correspond to the reflections of the FCC phase of metallic gold nanoparticles. This result clearly demonstrates that the bio-fabricated gold nanoparticles made from acai berry (AB) and bay leaf (BL) extracts are crystalline.

Using Debye-equation Scherrer's (formula 1), the average sizes of the diverse nanostructures were estimated to be 16 nm for AB and 12 nm for BL by calculating the width of the (111) reflection, which are consistent with TEM measurement.

$$D = \frac{K\lambda}{\beta s \cos\theta}$$

Formula 1. Debye-Scherrer’s equation.

According to the formula 1, D is the average crystallite size, where K is the Scherrer's constant of the true crystallite shape (0.94 is used to link spherical crystallites with cubic symmetry), λ is the wavelength of the XRD radiation (=1.5406), βs is the peak's full width and theta is the angle of diffraction.

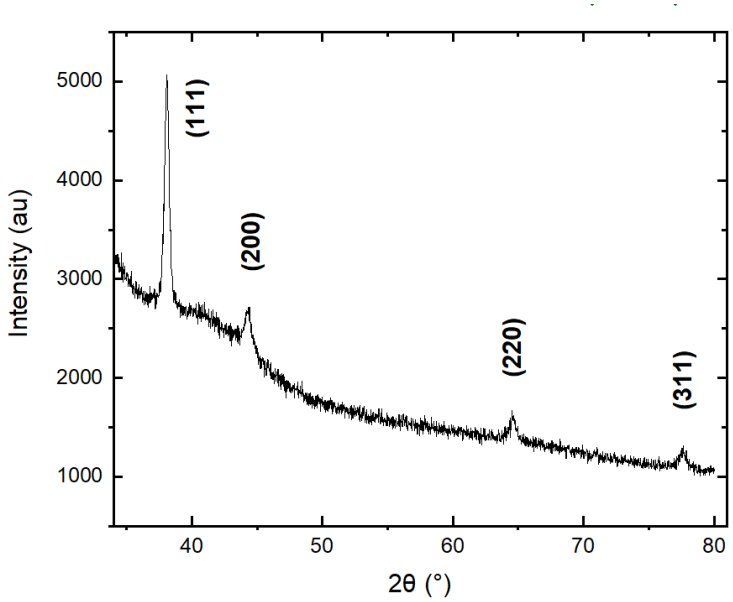

Figure 14. The XRD data of dried Au NPs fabricated by the extract of acai berry.

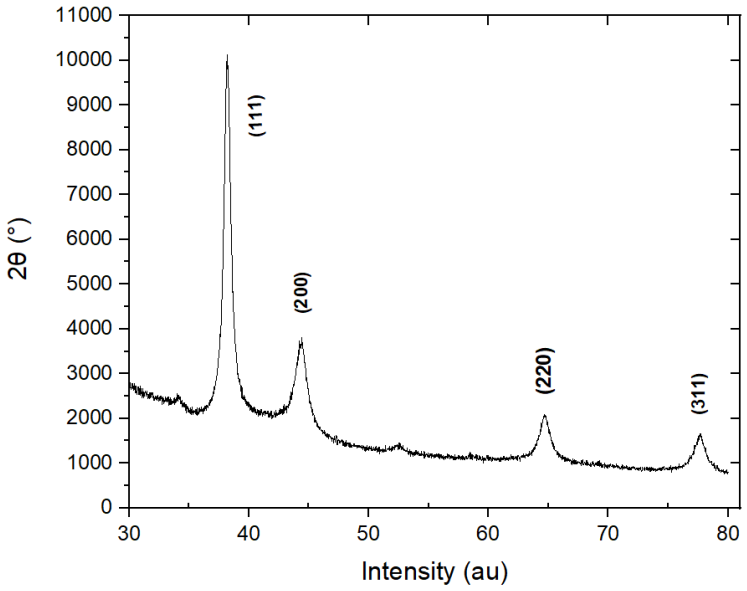

Figure 15. The XRD data of dried Au NPs fabricated by the extract of bay leaves.

4.2 UV-VIS Study of Acai Berry Gold Nanoparticles

UV-vis was used to confirm the LSPR wavelength of Au NPs (figure 17). The intensity of the g1 sample (5 ml) was lower than the intensity of g2 (10 ml); however, the g3 sample (15 ml) was higher than both samples. Nevertheless, all samples had the same LSPR peak at about 520 nm, resulting in intense violet color which does not present in the big-sized material (figure 16). The higher quantity of AB extract, the smaller the Au NPs, which will increase the Au NPs surface of contact with the UV-vis radiation, resulting in the variation in the intensity of the samples, where the g3 sample contains the smallest Au NPs, the g2 sample includes the intermediate Au NPs, and the g1 sample contains the biggest Au NPs. However, since the nanoparticles present in all the samples are made of gold under the same conditions, that is why they all had the same LSPR peak. Noting that the sharp peak indicates the formation of spherical Au NPs.

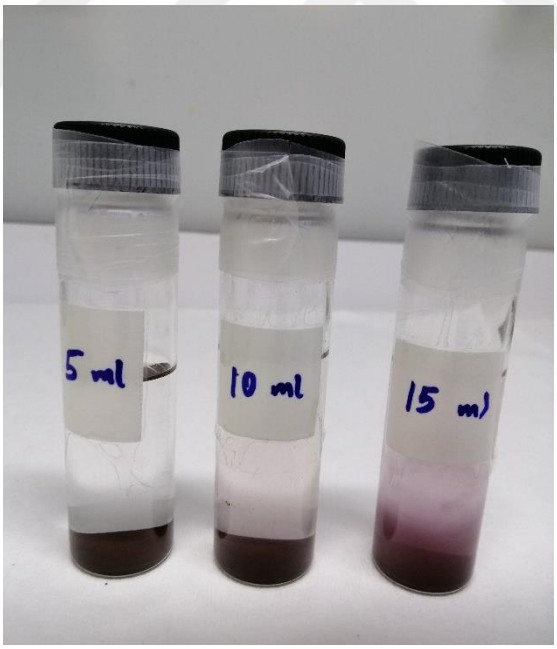

Figure 16. The deep violet color of the colloidal solutions of Au NPs synthesized by using acai berry.

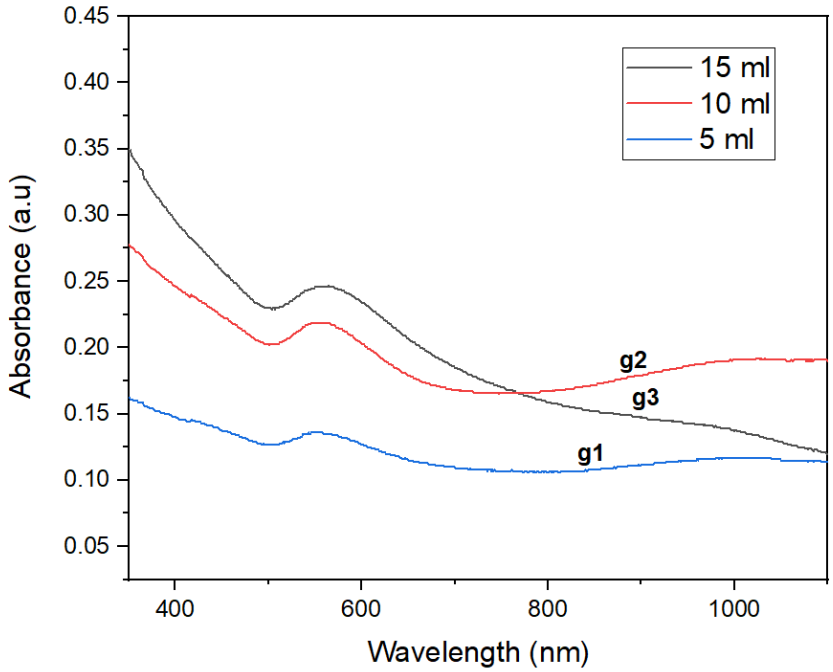

Figure 17. UV-visible absorption spectra of AB-Au NPs fabricated from diverse extract volumes (g1, g2, and g3).

4.3 TEM Analysis of Gold Nanoparticles Synthesized by Using Acai Berry and Bay Leaves

The Au NPs were characterized by TEM analysis. TEM images of green synthesized AuNPs with different extracts were observed in Figures 18 and 20. The formation of spherical shape gold nanoparticles (g2) from acai berry extract is visible in figure 16 with an average size of 16 nm. It is worth noting that most of the gold nanoparticles are well-separated. The size distribution of acai berry-Au nanoparticles is represented in a histogram which shows the variation in the particle size (figure 19). The average particle size was determined by measuring the diameter of 30 different particles to be approximately 22 ± 6 nm, which is consistent with the mean crystal size calculated from the Scherrer equation (formula 1).

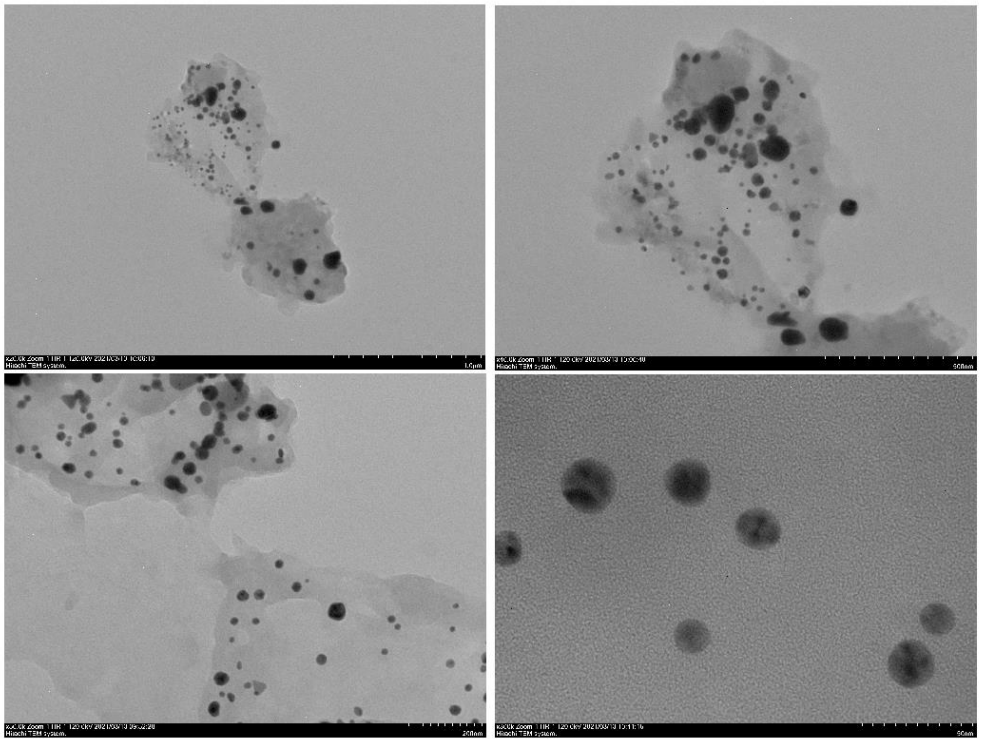

Figure 18. TEM images of colloidal acai berry-gold nanoparticles (g2) under different magnification.

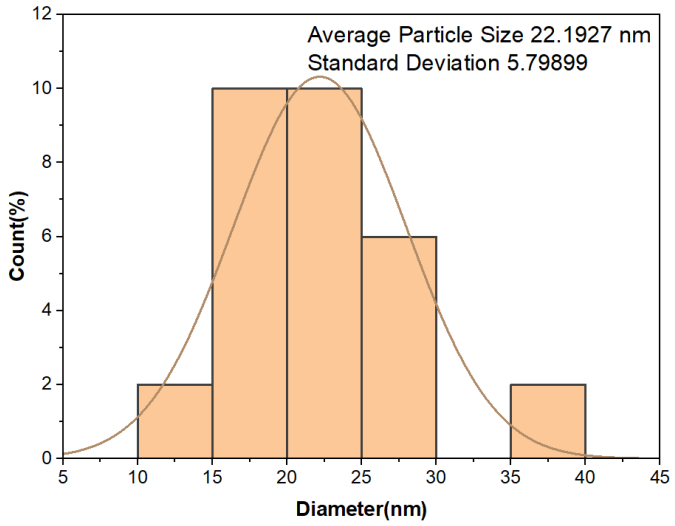

Figure 19. The size distribution of acai berry-Au nanoparticles.

TEM images of bay leaves-Au NPs consist of many spherical shapes with a small number of multi-branched gold nanoparticles (figure 20). Triangular and rod-

like gold nanoparticles could also be seen in figure 21. The particles are almost spherical ad the average size of 16 nm. The high-resolution TEM image reveals clear lattice fringes with a separation distance of 0.23 nm, which corresponds to the (111) plane of FCC gold (Figure 22). The lattice fringes of acai berry-Au NPs have not been provided due to the lack of high-resolution TEM images.

The particle size distribution was evaluated by observing the diameter of 30 different particles and was found to be 346 nm, which agrees with the mean crystal size calculated from the Scherrer equation (figure 23). Notably, the different sizes of the NPs from different extracts could be the result of the quantity of reducing agents in the plant extracts or different phytochemicals involved in the synthesis.

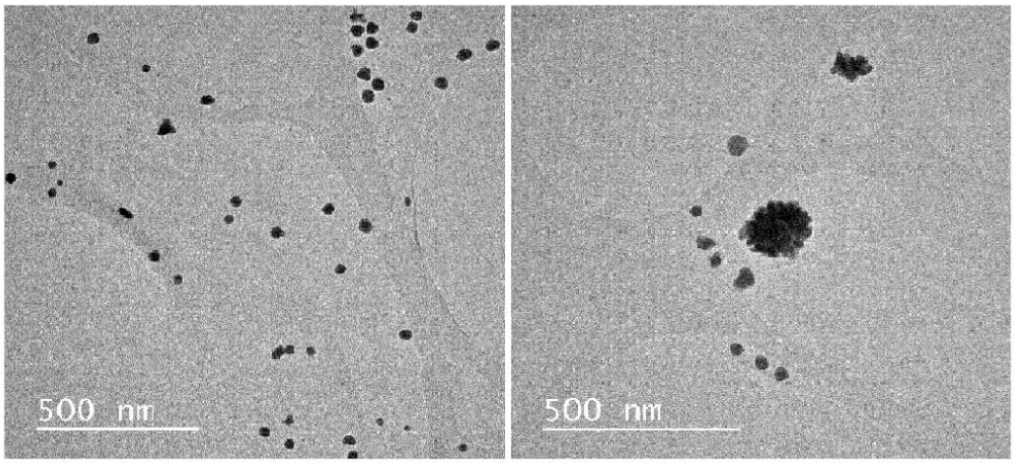

Figure 20. TEM images of spherical and multi-branched shapes of bay leaves-Au NPs.

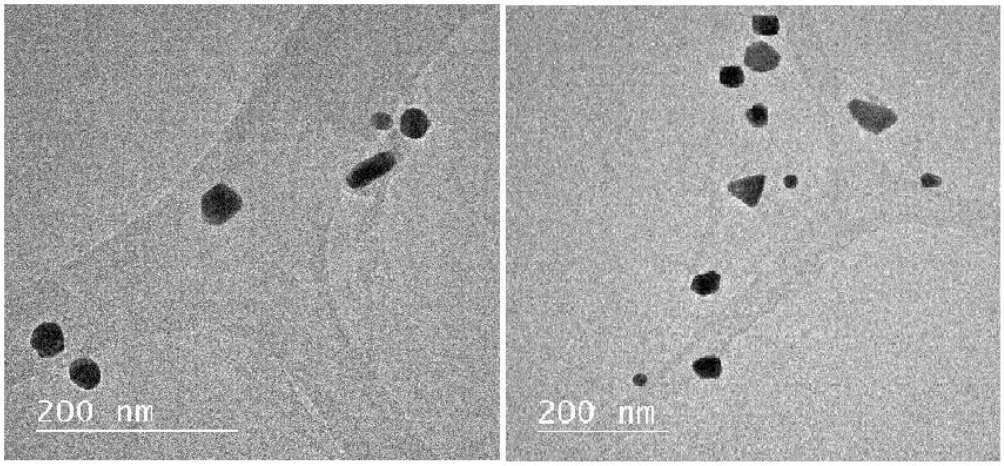

Figure 21. TEM images of rod-like and triangular shapes of bay leaves-Au NPs.

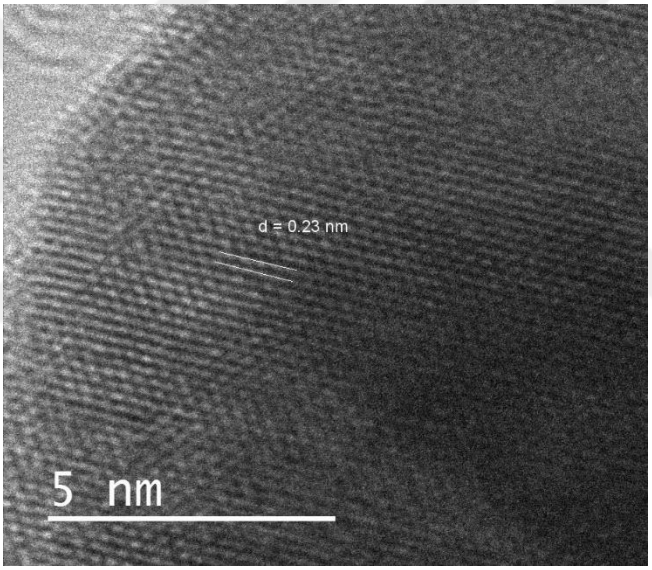

Figure 22. Lattice fringes of single Au nanocrystal with a spacing of 0.23 nm.

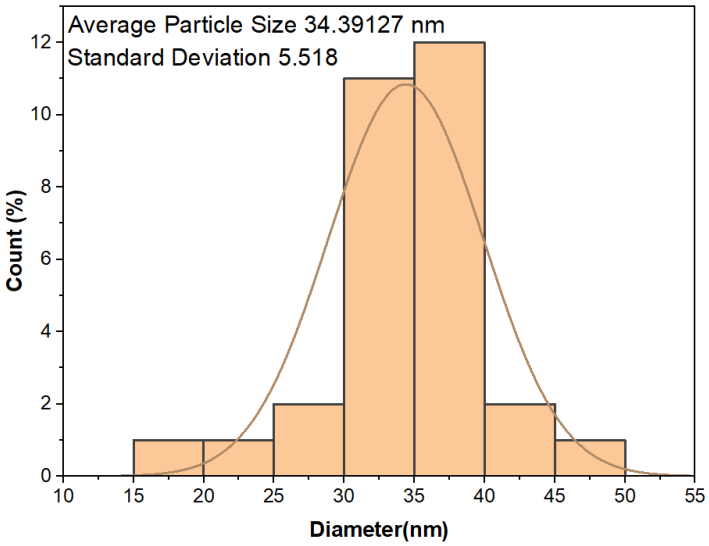

Figure 23. The size distribution of bay leaves-Au nanoparticles.

4.4 FTIR Result of Acai Berry Gold Nanoparticles

Fourier-Transform Infrared Spectroscopy (FTIR) is a major biological instrument in which the main role is the identification of chemical interactions in a particular molecule. However, the reduction and capping of Au ions are maintained by biomolecules. The FTIR spectrum of *E. oleracea*'s extract (figure 5) revealed peaks at 3,576 (O-H stretch of alcohols/phenols), 1741 (−C=C– the stretch of alkynes), and 1,466 cm^{-1} (C-N compounds and C-O-C bond). Additionally, the C-O and C-O-C stretch of primary alcohol and phenolic compounds appear at around 1,162 cm^{-1}.

The main differences shown between the raw material spectra and the as-prepared Au NPs spectra are the modifications that occurred in the (-COOH) group for -OH, i.e., a hydroxyl group. After Au NPs reduction, the peak reached 3,262 cm^{-1} in synthesized nanoparticles compared to the peak in raw material, where it was at 3,576 cm^{-1}. In this scenario, the peak of nanoparticles became narrower with less intensity. The 1,443 cm^{-1} was contributed to the C-N compounds and C-O-C bond.

The conversion of the (-OH group) to aldehyde was indicated through the reduction of the 1741 cm^{-1} and 1466 cm^{-1} peaks to 1625 cm^{-1}. Moreover, the ability of protein's peptides and amino acid's CO group to bind metal was revealed through the

obtained peaks shown in the range from 1075 to 1625 cm^{-1} in the IR band of fabricated Au NPs. This indicates that the proteins most likely formed a coating layer on the AuNPs, preventing particle aggregation.

These obtained results are consistent with Lima et al. findings. (Lima et al.,2012) They discovered the *E. oleracea* FT-IR spectrum to start from 500 to 4000 cm^{-1}, which confirms the existence of diverse phytochemicals for generating and stabilizing of Au NPs.

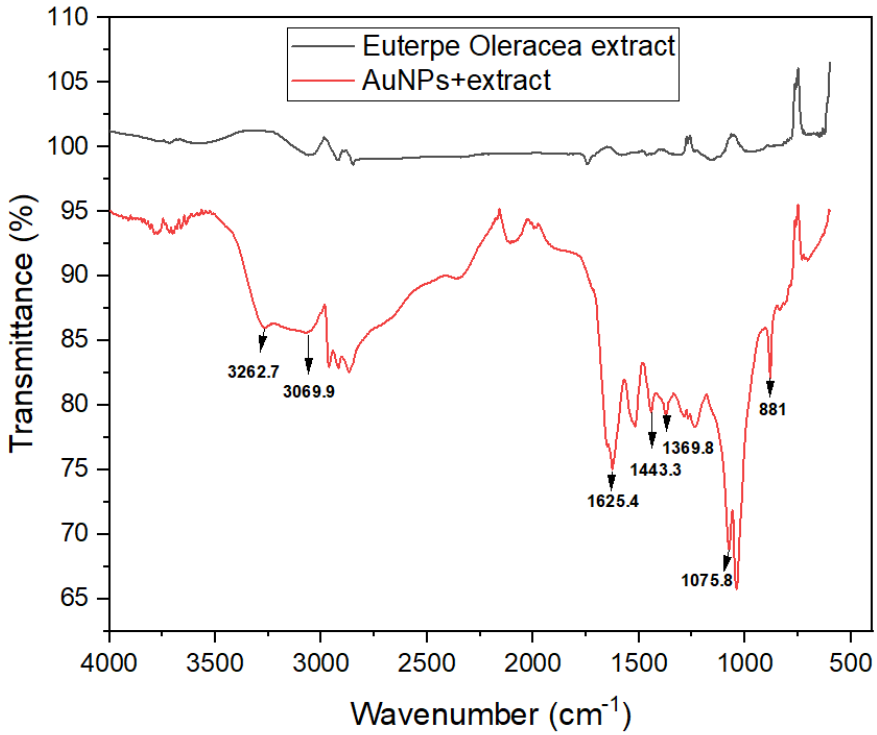

Figure 24. FTIR data of gold nanoparticles.

4.5 ICP-OES Analysis for Gold Nanoparticles Synthesized By Using Acai Berry and Bay Leaves

Inductively Coupled Plasma Emission Spectrometry (ICP) was used to calculate the percentage conversion of metal ions to metal nanoparticles.

$$Q=(C0-Cf)/C0\times100$$

Formula 2. The percentage of metal ions transformed into nanoparticles.

In this equation, the initial and final concentrations of metal ions have been determined with C0 and Cf (23,630 mg/L, 0.072 mg/L) and (23,630 mg/L, 0.045 mg/L) for acai berry-Au NPs (AB) and bay leaves-Au NPs (BL), respectively. Q is the percentage conversion of gold ions to gold nanoparticles.

The final synthetic yield of Au NPs was determined to be 99.69 % and 99.8 % for AB and BL, respectively:

Q (AB) = 99.69 %

Q (BL)= 99.8 %

4.6 Hydrogel-based Gold Swimmers

The hydrogel is prepared by blending gelatin, alginate, and cellulose in a weight ratio of 5:2:2 and dissolving the mixture in distilled water. The solution is thoroughly mixed for one hour at 60°C using a magnetic stirrer until the solution attains proper homogeneity. The mixture is kept in the fridge at 4°C until it reaches a gel-like consistency. The gold swimmers are then synthesized by mixing pre-synthesized gold nanoparticles (acai-berry) with the hydrogel solution and dropping them into a $CaCl_2$ bath with the help of an extrusion-based 3d printer as shown in figure 25. Synthesis tests showed that 1% wt/vol concentration is the best for ease of printability when coupled with a 0.3mm printing nozzle and at a 1.47 mm^3/s extrusion speed. After drying the gold swimmers shrunk down to micrometer diameter. This shrinkage in size is due to the loss of water content from the hydrogel, which accounts for 99.5 percent of the overall solution. After the preparation, these swimmers did not exhibit photo response to the visible light incident in a medium contains H_2O_2. The reason for this could be the plasmons not being able to get interacted with fuel solution because of the hydrogel-based enclosing.

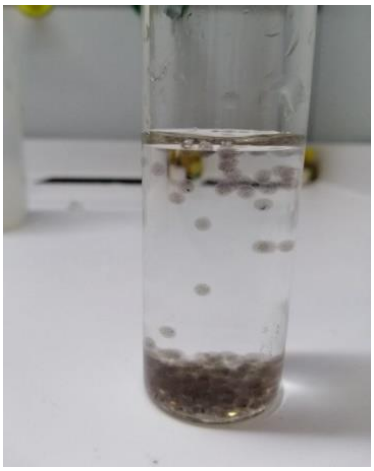

Figure 25. The hydrogel-based gold swimmers.

4.7 Resin-based Gold Swimmers

Acai berry-gold nanoparticles with photocatalytic properties were mixed with the photocurable polymer resin, which is the primary material in the sub-milli and milli-swimmers produced. A 0.1% wt/vol concentration was obtained by mixing 0.0267 g of gold nanoparticles and 20 ml of polymer resin for each gold particle-resin combination. The mixture was sonicated for 30 minutes before beginning the printing process to help stop the gold nanoparticles from integrating. . The resulting mixture was poured into the tank, and the build platform was settled to print the structures. The particles were designed by using CAD software. After the printing process, the swimmers were cleaned with <99% pure ethanol for 3 minutes to remove the unpolymerized resin. Following the synthesizing, they were submerged in hydrogen peroxide (H_2O_2) as a fuel liquid under the xenon visible light effect, but we did not notice any movement. The reason for this could be the plasmons not being able to get interacted with fuel solution because of the resin based enclosing.

4.8 Plasmonic Self-propelled Gold Nanoparticles

Gold nanoparticles having an elevated surface-to-volume ratio and a high number of active catalytic sites per unit area make them ideal candidates for superior

catalytic performance. Moreover, the localized surface plasmon resonance (LSPR) effect and strong visible absorption could be utilized to self-propel nanostructures.

This photocatalytic activity arises when gold nanoparticles are irradiated by a xenon lamp. Visible light at a certain wavelength excites the surface plasmon resonance to work as a light harvester. The excitation of Au NPs LSPR leads to an interband excitation of electrons from the occupied 5d band to the upper conduction band (6sp). Therefore, excited hot electrons can be formed on the metal surface from direct excitation using visible illumination. These hot electrons can transfer into an electron acceptor, adsorbed on the metal surface, inducing a chemical decomposition reaction. figure 26 and formula 3.

$$\text{Photocatalyst} \rightarrow e_{CB}^{-} + h_{VB}^{+}$$

Formula 3. Electron-hole pair

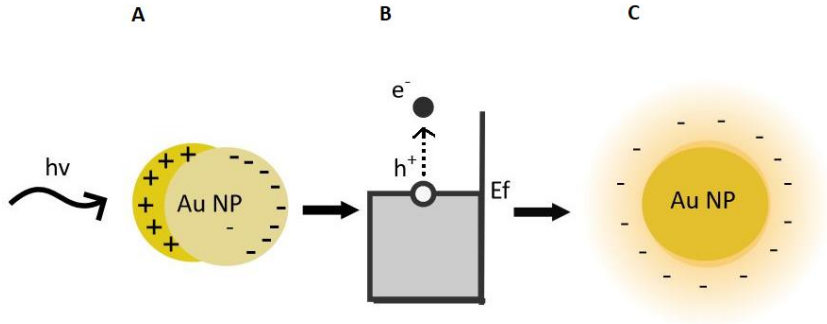

Figure 26. Schematics of plasmon induced-hot electrons generation on Au NP (A and C) and inter-band structure of photocatalyst phase (B).

The catalytically driven propulsion of gold nanostructures can be explained with the following formula:

$$2\ H_2O_2 \rightarrow 2\ H_2O + 2\ O_2 \uparrow$$

Formula 4. Catalytic decomposition of Hydrogen peroxide.

Ergo, the release of oxygen bubbles is caused by the chemical decomposition of H_2O_2 is an indication that the reaction is taking place. In parallel with a result obtained from a previous study. Au NPs' movement towards visible light can be explained by the electrostatic interaction of the electrons present on the surface of the nanoparticles and the hydrogen atoms of the hydrogen peroxide molecules. Because electrons are not equally shared between the hydrogen and the oxygen atoms in the hydrogen peroxide molecules, since oxygen is more electronegative than hydrogen, electrons are attracted towards the oxygen atom creating a quasi-negative (δ^-) charge on the oxygen atom and a quasi-positive charge (δ^+) on the hydrogen atom (Sridhar et al., 2018). (Figure 13), and the velocities of the Au NPs are dependent on the H_2O_2 fuel concentration as will be shown in the next section.

4.8.1 Trajectory and speed analysis of plasmonic self-propelled gold nano-swimmers. Au NPs present in 10% of the reducing agent were used for the following experiments. To investigate the impact of H2O2 concentration on the acceleration of AB-Au NPs, three various amounts of this fuel solution were used. For each concentration, the speed ratios of three different nanoparticles were calculated to evaluate the average speed value. However, the light intensity was kept constant for various H2O2 concentrations, including 2%, 4%, and 6% at 35W. The resulting travel speed of the nanoparticles towards the source of light increased with the rise of the H2O2 concentration (tracked for 12 seconds). (figure 27 - 30).

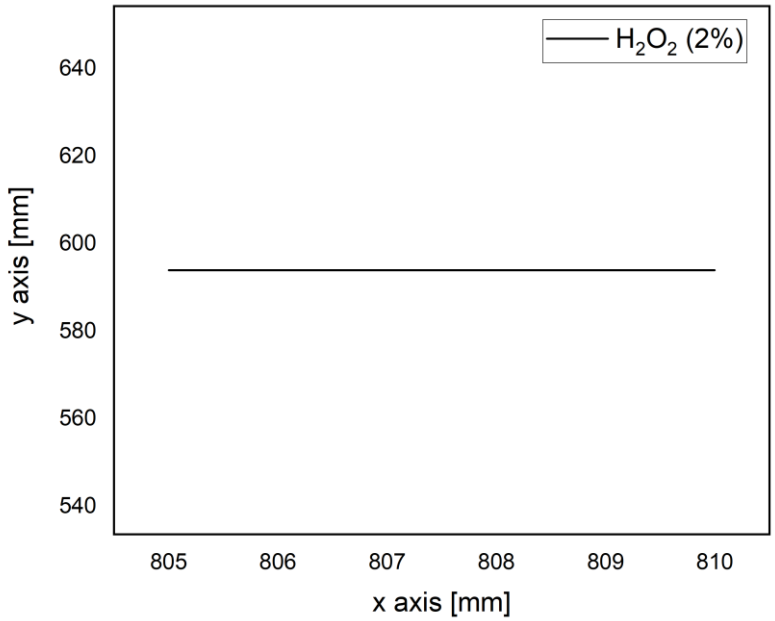

Figure 27. The swimming trajectory of gold nanoparticles under external visible electromagnetic guidance in 2% H_2O_2 concentration.

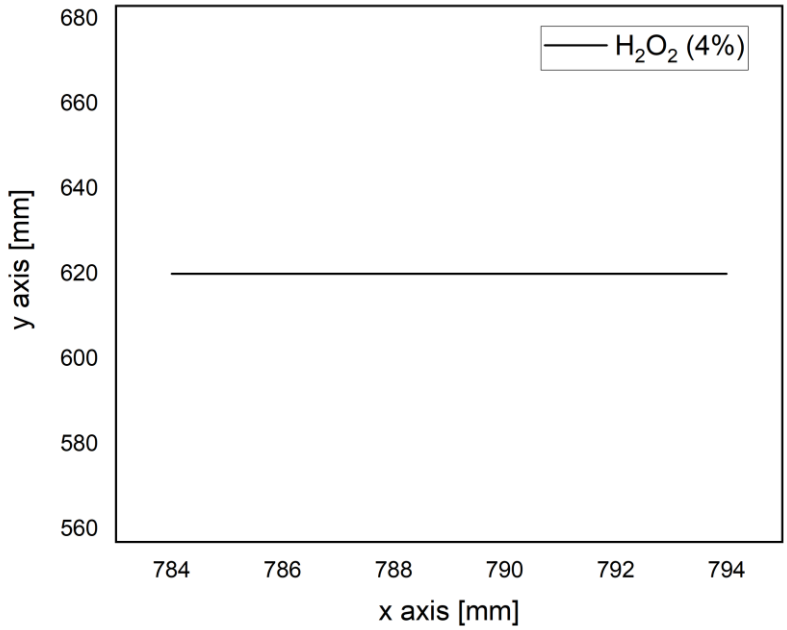

Figure 28. The swimming trajectory of gold nanoparticles under external visible electromagnetic guidance in 4% H_2O_2 concentration.

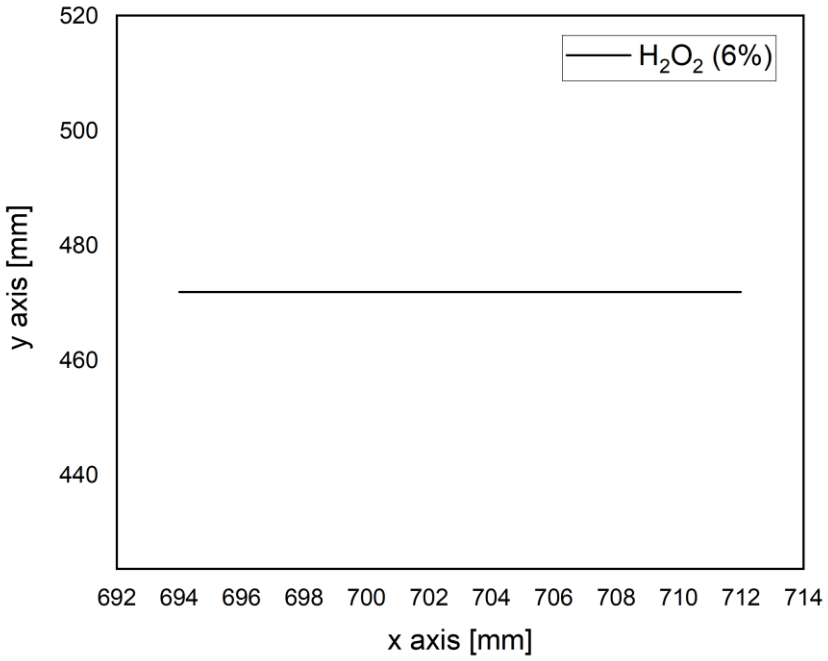

Figure 29. The swimming trajectory of gold nanoparticles under external visible electromagnetic guidance in 6% H_2O_2 concentration.

The average speeds of the biosynthesized gold nanoparticles are estimated to be 0.00435 mm s^{-1}, 0.011 mm s^{-1}, and 0.017699 mm s^{-1} for 2%, 4%, and 6% H_2O_2 concentration, respectively. The migration of the gold nanoparticles towards the light source was observed to be a straight line.

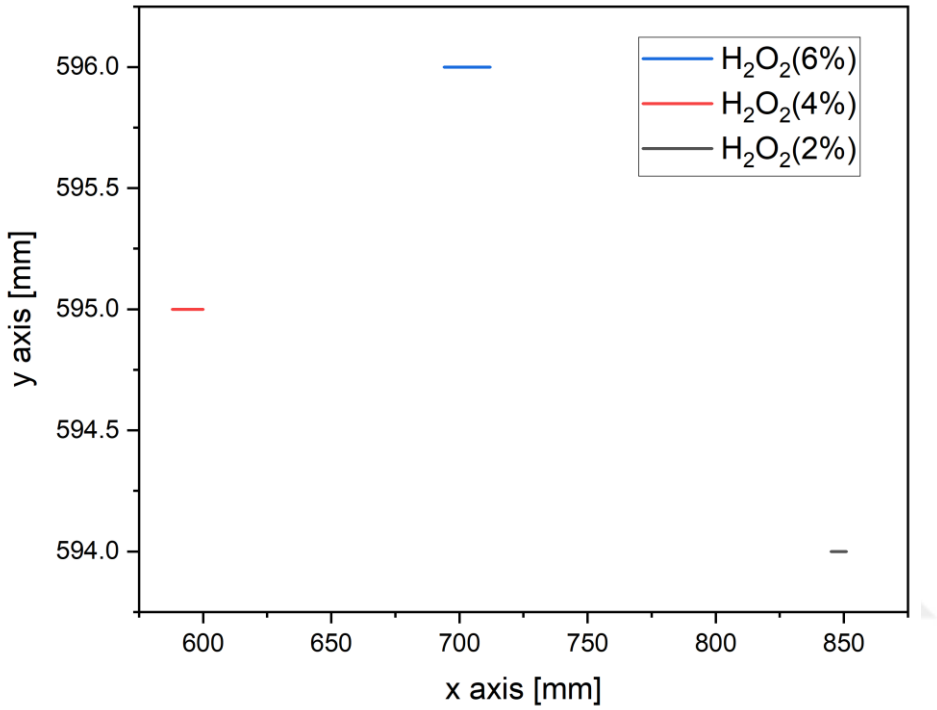

Figure 30. Dependence of the average speed of gold nanoparticles on H_2O_2 concentration under external visible light source

Only when exposed to VIS xenon light, which acts as a force, do these gold nanoparticles move. Self-generated active propulsion occurs only when the (xenon) VIS light is lit. When the VIS light is turned off, the particles' active propulsion stops, and they only move in a random Brownian motion.

In our case, the temperature of the medium is one of our biggest concerns. By tracking the temperature throughout the reaction, we observed that there was no conspicuous change between the initial and final temperature. Therefore, we can confirm that the motion is not caused by the increase of the medium temperature.

In comparison to previous studies, many of them have produced metal oxide-based nanostructures such as TiO_2 (Sridhar et al., 2018), Cu_2O (Zhou et al., 2017), WO_3 (Zhang et al., 2017), and Si (Wang et al., 2017), to produce self-propulsion nanomotors. Some of them have produced self-powered polymer multilayer Janus capsules by deposition a thin gold layer on the polymer. (Wu et al., 2014) In all of them, the travel speed could be monitored by the fuel concentration and the navigation could be directed by either an external magnetic field or electromagnetic field.

In our work, we provided a feasible gold nanoparticles formation method for self-driven gold nanoparticles with elevated swimming speed and positional guidance without the use of any additional material

4.9 Future Work

In our present study, we used the method of green chemistry to produce monodisperse gold nanoparticles in shape uniformity, which showed an efficient photocatalytic activity. Such programmed behavior that links the response to external electromagnetic field (light response) and concentration gradients of chemicals were able to produce directional self-propelled nanomotors.

In future work, the ability to introduce a powerful biocompatible fuel solution will be a better option and open the on-hand possibility to develop driven-nanomotors in a nontoxic environment. The intensive research on the catalysis of Au NPs for various reactions is constantly continued, due to the large surface to volume ratio and controllable motion under the visible light effect. We anticipate that the combination of offering suitable force liquid and Au NP-based plasmonic photocatalysts will result in the further development of numerous processes. Making these nanostructures as carriers by loading several substances like biomolecules and drugs for targeted drug delivery and other medical applications.

Chapter 5
Conclusion

By reducing aqueous AuCl4- ions with bioactive compounds, Au NPs were created using a green chemistry concept. found in plant extracts of acai berry and bay leaves. The synthesized AuNPs were characterized using a multy instrumental techniques which are UV–vis, TEM, XRD, FTIR, and ICP. The generated gold nanoparticles shape was majorly spherical in case of acai berry NPs and bay leaves NPs. Moreover, the mean size of AB-Au NPs and BL- NPs were obtained to be 16 and 12 nm, respectively.

In summary, we have presented a driven catalytically powered nanomotor from acai berry-Au NPs. These nanomotors could be driven by the electrostatic interaction resulted from the catalytic decomposition of hydrogen peroxide on Au NPs surface under xenon light. Their velocities were measured under various concentrations of the fuel liquid (H_2O_2). As the concentration of H_2O_2 increased, the nanoparticles travel speed towards the source of light enhanced. This effect would result from the excellent photocatalytic activity of the Au metal. Developed Au swimmers could be used in next generation photo assisted drug delivery applications.

REFERENCES

Books

Laguna, A. (2008). Modern supramolecular gold chemistry: gold-metal interactions and applications. Wiley-VCH.

Kanchi, S., & Ahmed, S. (2018). Green metal nanoparticles: Synthesis, characterization and their applications. Wiley, Scrivener Publishing.

Balasooriya, E. R., Jayasinghe, C. D., Jayawardena, U. A., Ruwanthika, R. W., Mendis de Silva, R., & Udagama, P. V. (2017). Honey mediated green synthesis of nanoparticles:

Choudhary, D. K., Varma, A., Bhargava, P., & Ghorbanpour, M. (2020). Biogenic nano-particles and their use in agro-ecosystems. Springer.

Periodicals

Hamelian, M., Hemmati, S., Varmira, K., & Veisi, H. (2018). Green synthesis, antibacterial, antioxidant and cytotoxic effect of gold nanoparticles using pistacia Atlantica Extract. Journal of the Taiwan Institute of Chemical Engineers, 93, 21-30. doi:10.1016/j.jtice.2018.07.018

Dubey, S. P., Lahtinen, M., & Sillanpää, M. (2010). Green synthesis and characterizations of silver and gold nanoparticles Using leaf extract of Rosa rugosa. Colloids and Surfaces A: Physicochemical and Engineering Aspects, 364(1-3), 34-41. doi:10.1016/j.colsurfa.2010.04.023

KSV, G. (2017). Green synthesis of Iron nanoparticles using green tea leaves extract. Journal of Nanomedicine & Biotherapeutic Discovery, 07(01). doi:10.4172/2155-983x.1000151

Geetha, R., Ashokkumar, T., Tamilselvan, S., Govindaraju, K., Sadiq, M., & Singaravelu, G. (2013). Green synthesis of gold nanoparticles and their anticancer activity. Cancer Nanotechnology, 4(4-5), 91-98. doi:10.1007/s12645-013-0040-9

Gericke, M., & Pinches, A. (2006). Biological synthesis of metal nanoparticles. Hydrometallurgy, 83(1-4), 132-140. doi:10.1016/j.hydromet.2006.03.019

Phiri, M. M., Mulder, D. W., & Vorster, B. C. (2019). Seedless gold Nanostars WITH SEED-LIKE advantages for Biosensing applications. Royal Society Open Science, 6(2), 181971. https://doi.org/10.1098/rsos.181971

Draz, M. S., & Shafiee, H. (2018). Applications of gold nanoparticles in virus detection. Theranostics, 8(7), 1985–2017. https://doi.org/10.7150/thno.23856

Garg, N., Bera, S., Rastogi, L., Ballal, A., & Balaramakrishna, M. V. (2020). Synthesis and characterization of l-asparagine stabilised gold nanoparticles: Catalyst for degradation of organic dyes. Spectrochimica Acta Part A: Molecular and Biomolecular Spectroscopy, 232, 118126. https://doi.org/10.1016/j.saa.2020.118126

Malarkodi, C., Rajeshkumar, S., & Annadurai, G. (2017). Detection of environmentally hazardous pesticide in fruit and vegetable samples using gold

nanoparticles. Food Control, 80, 11–18. https://doi.org/10.1016/j.foodcont.2017.04.023

Cho, J.-H., Kim, A.-R., Kim, S.-H., Lee, S.-J., Chung, H., & Yoon, M.-Y. (2017). Development of a novel imaging agent using peptide-coated gold nanoparticles toward brain glioma stem cell marker cd133. Acta Biomaterialia, 47, 182–192. https://doi.org/10.1016/j.actbio.2016.10.009

Zeiri, Y., Elia, P., Zach, R., Hazan, S., Kolusheva, S., & Porat, Z. (2014). Green synthesis of gold nanoparticles using plant extracts as reducing agents. International Journal of Nanomedicine, 4007. doi:10.2147/ijn.s57343

Taylor, P., Biswas, P., & Wu, C. (2012). Journal of the Air & Waste Management Nanoparticles and the Environment Nanoparticles and the Environment, (January 2013), 37–41.

Batacharyya et. al. (1995). Bhattacharyya et al.pdf, 9(24), 3489–3493.

Dubchak, S., Ogar, A., Mietelski, J. W., & Turnau, K. (2010). Influence of silver and titanium nanoparticles on arbuscular mycorrhiza colonization and accumulation of radiocaesium in Helianthus annuus. Spanish Journal of Agricultural Research, 8(SPL ISS.), 103–108. https://doi.org/10.5424/sjar/201008s1-1228

Sharma, V. K., Yngard, R. A., & Lin, Y. (2009). Silver nanoparticles: Green synthesis and their antimicrobial activities. Advances in Colloid and Interface Science, 145(1–2), 83–96. https://doi.org/10.1016/j.cis.2008.09.002

Kowalczyk, B., Lagzi, I., & Grzybowski, B. A. (2011). Nanoseparations: Strategies for size and/or shape-selective purification of nanoparticles. Current Opinion in Colloid and Interface Science, 16(2), 135–148. https://doi.org/10.1016/j.cocis.2011.01.004

Vijayakumar, S., Vaseeharan, B., Malaikozhundan, B., & Shobiya, M. (2016). Laurus nobilis leaf extract mediated green synthesis of ZnO nanoparticles: Characterization and biomedical applications. Biomedicine and Pharmacotherapy, 84, 1213–1222. https://doi.org/10.1016/j.biopha.2016.10.038

Schmidbaur, H., Cronje, S., Djordjevic, B., & Schuster, O. (2005). Understanding gold chemistry through relativity. Chemical Physics, 311(1-2 SPEC.ISS.), 151–161. https://doi.org/10.1016/j.chemphys.2004.09.023

Cai, W. (2008). Applications of gold nanoparticles in cancer nanotechnology. Nanotechnology, Science and Applications, Volume 1, 17–32. https://doi.org/10.2147/nsa.s3788

Tang, D., Yuan, R., & Chai, Y. (2007). Biochemical and immunochemical characterization of the antigen–antibody reaction on a non-toxic biomimetic interface immobilized red blood cells of crucian carp and gold nanoparticles. Biosensors and Bioelectronics, 22(6), 1116–1120. https://doi.org/10.1016/j.bios.2006.04.031

Medley, C. D., Smith, J. E., Tang, Z., Wu, Y., Bamrungsap, S., & Tan, W. (2008). Gold Nanoparticle-Based Colorimetric Assay for the Direct Detection of Cancerous Cells. Analytical Chemistry, 80(4), 1067–1072. https://doi.org/10.1021/ac702037y

Liu, X., Dai, Q., Austin, L., Coutts, J., Knowles, G., Zou, J., Chen, H., & Huo, Q. (2008). A One-Step Homogeneous Immunoassay for Cancer Biomarker Detection Using Gold Nanoparticle Probes Coupled with Dynamic Light Scattering. Journal of the American Chemical Society, 130(9), 2780–2782. https://doi.org/10.1021/ja711298b

Louis, C., & Pluchery, O. (2012). Gold nanoparticles for physics, Chemistry and Biology. World Scientific.

Zeng, C., & Jin, R. (2014). Gold nanoclusters: Size-controlled synthesis and crystal structures. Structure and Bonding, 87–115. https://doi.org/10.1007/430_2014_146

Ghasemi-Mobarakeh, L., Kolahreez, D., Ramakrishna, S., & Williams, D. (2019). Key terminology in biomaterials and biocompatibility. Current Opinion in Biomedical Engineering, 10, 45–50. https://doi.org/10.1016/j.cobme.2019.02.004

Connor, E. E., Mwamuka, J., Gole, A., Murphy, C. J., & Wyatt, M. D. (2005). Gold Nanoparticles Are Taken Up by Human Cells but Do Not Cause Acute Cytotoxicity. Small, 1(3), 325–327. https://doi.org/10.1002/smll.200400093

Gannon, C. J., Patra, C., Bhattacharya, R., Mukherjee, P., & Curley, S. A. (2008). Intracellular gold nanoparticles enhance non-invasive radiofrequency thermal destruction of human gastrointestinal cancer cells. Journal of Nanobiotechnology, 6(1), 2. https://doi.org/10.1186/1477-3155-6-2

Shukla, R., Bansal, V., Chaudhary, M., Basu, A., Bhonde, R. R., & Sastry, M. (2005). Biocompatibility of Gold Nanoparticles and Their Endocytotic Fate Inside the Cellular Compartment: A Microscopic Overview. Langmuir, 21(23), 10644–10654. https://doi.org/10.1021/la0513712

Smitha, S. L., Philip, D., & Gopchandran, K. G. (2009). Green synthesis of gold nanoparticles using cinnamomum zeylanicum leaf broth. Spectrochimica Acta Part A: Molecular and Biomolecular Spectroscopy, 74(3), 735–739. https://doi.org/10.1016/j.saa.2009.08.007

Ananda Chitra, M. (2016). Rapid Detection of Staphylococcus aureus Genomic DNA Using Peptide Nucleic Acid and Gold Nanoparticles. Proceedings of the National Academy of Sciences, India Section B: Biological Sciences, 88(2), 803–811. https://doi.org/10.1007/s40011-016-0820-1

Safavi, A., Absalan, G., & Bamdad, F. (2008). Effect of gold nanoparticle as a novel nanocatalyst on luminol–hydrazine chemiluminescence system and its analytical application. Analytica Chimica Acta, 610(2), 243–248. https://doi.org/10.1016/j.aca.2008.01.053

Yaqoob, S. B., Adnan, R., Rameez Khan, R. M., & Rashid, M. (2020). Gold, Silver, and Palladium Nanoparticles: A Chemical Tool for Biomedical Applications. Frontiers in Chemistry, 8. https://doi.org/10.3389/fchem.2020.00376

Jain, P. K., Lee, K. S., El-Sayed, I. H., & El-Sayed, M. A. (2006). Calculated absorption and scattering properties of gold nanoparticles of different size, shape, and composition: applications in Biological Imaging and biomedicine. The Journal of Physical Chemistry B, 110(14), 7238–7248. https://doi.org/10.1021/jp057170o

Daniel, M.-C., & Astruc, D. (2004). Gold Nanoparticles: Assembly, Supramolecular Chemistry, Quantum-Size-Related Properties, and Applications toward Biology,

Catalysis, and Nanotechnology. Chemical Reviews, 104(1), 293–346. https://doi.org/10.1021/cr030698+

Link, S., & El-Sayed, M. A. (2000). Shape and size dependence of radiative, non-radiative and photothermal properties of gold nanocrystals. International Reviews in Physical Chemistry, 19(3), 409–453. https://doi.org/10.1080/01442350050034180

El-Brolossy, T. A., Abdallah, T., Mohamed, M. B., Abdallah, S., Easawi, K., Negm, S., & Talaat, H. (2008). Shape and size dependence of the surface plasmon resonance of gold nanoparticles studied by Photoacoustic technique. The European Physical Journal Special Topics, 153(1), 361–364. https://doi.org/10.1140/epjst/e2008-00462-0

Zhuang, Y., Liu, L., Wu, X., Tian, Y., Zhou, X., Xu, S., Xie, Z., & Ma, Y. (2018). Size and Shape Effect of Gold Nanoparticles in "Far-Field" Surface Plasmon Resonance. Particle & Particle Systems Characterization, 36(1), 1800077. https://doi.org/10.1002/ppsc.201800077

Balasubramanian, S. K., Yang, L., Yung, L.-Y. L., Ong, C.-N., Ong, W.-Y., & Yu, L. E. (2010). Characterization, purification, and stability of gold nanoparticles. Biomaterials, 31(34), 9023–9030. https://doi.org/10.1016/j.biomaterials.2010.08.012

Zhang, H., Chen, G., & Bahnemann, D. W. (2009). Photoelectrocatalytic materials for environmental applications. Journal of Materials Chemistry, 19(29), 5089. https://doi.org/10.1039/b821991e

Curti, M., Bahnemann, D. W., & Mendive, C. B. (2016). Mechanisms in heterogeneous photocatalysis: Titania under UV and visible light illumination.

Wang, Y.-S., Xia, H., Lv, C., Wang, L., Dong, W.-F., Feng, J., & Sun, H.-B. (2015). Self-propelled micromotors based on au–mesoporous silica nanorods. Nanoscale, 7(28), 11951–11955. https://doi.org/10.1039/c5nr02545a

Mateo, D., Esteve-Adell, I., Albero, J., Royo, J. F., Primo, A., & Garcia, H. (2016). 111 oriented gold nanoplatelets on multilayer graphene as visible light photocatalyst for overall water splitting. Nature Communications, 7(1). https://doi.org/10.1038/ncomms11819

Reference Module in Materials Science and Materials Engineering. https://doi.org/10.1016/b978-0-12-803581-8.03800-5

Loget, G., & Kuhn, A. (2011). Electric field-induced chemical locomotion of conducting objects. Nature Communications, 2(1). https://doi.org/10.1038/ncomms1550

Dreyfus, R., Baudry, J., Roper, M. L., Fermigier, M., Stone, H. A., & Bibette, J. (2005). Microscopic artificial swimmers. Nature, 437(7060), 862–865. https://doi.org/10.1038/nature04090

Orozco, J., Cheng, G., Vilela, D., Sattayasamitsathit, S., Vazquez-Duhalt, R., Valdés-Ramírez, G., Pak, O. S., Escarpa, A., Kan, C., & Wang, J. (2013). Micromotor-based high-yielding fast oxidative detoxification of chemical threats. Angewandte Chemie, 125(50), 13518–13521. https://doi.org/10.1002/ange.201308072

Patra, D., Sengupta, S., Duan, W., Zhang, H., Pavlick, R., & Sen, A. (2013). Intelligent, self-powered, Drug Delivery Systems. Nanoscale, 5(4), 1273–1283. https://doi.org/10.1039/c2nr32600k

Ceylan, H., Giltinan, J., Kozielski, K., & Sitti, M. (2017). Mobile microrobots for bioengineering applications. Lab on a Chip, 17(10), 1705–1724. https://doi.org/10.1039/c7lc00064b

Duan, W., Wang, W., Das, S., Yadav, V., Mallouk, T. E., & Sen, A. (2015). Synthetic nano- and micromachines in analytical chemistry: Sensing, migration, capture, delivery, and separation. Annual Review of Analytical Chemistry, 8(1), 311–333. https://doi.org/10.1146/annurev-anchem-071114-040125

Turkevich, J., Stevenson, P. C., & Hillier, J. (1951). A study of the nucleation and growth processes in the synthesis of colloidal gold. Discussions of the Faraday Society, 11, 55. https://doi.org/10.1039/df9511100055

Martin, C. R. (1996). Membrane-Based Synthesis of Nanomaterials. https://doi.org/10.21236/ada309882

Chu, M., & Wu. (2011). A gold nanoshell with a silica inner shell synthesized using liposome templates for doxorubicin loading and near-infrared photothermal therapy. International Journal of Nanomedicine, 807. https://doi.org/10.2147/ijn.s16701

Qiu, J., Xie, M., Wu, T., Qin, D., & Xia, Y. (2020). Gold nanocages for effective photothermal conversion and related applications. Chemical Science, 11(48), 12955–12973. https://doi.org/10.1039/d0sc05146b

Skrabalak, S. E., Chen, J., Sun, Y., Lu, X., Au, L., Cobley, C. M., & Xia, Y. (2008). Gold nanocages: Synthesis, properties, and applications. *Accounts of Chemical Research*, *41*(12), 1587–1595. https://doi.org/10.1021/ar800018v

Dahl, J. A., Maddux, B. L., & Hutchison, J. E. (2007). Toward greener nanosynthesis. Chemical Reviews, 107(6), 2228–2269. https://doi.org/10.1021/cr050943k

KSV, G. (2017). Green Synthesis of Iron Nanoparticles Using Green Tea leaves Extract. Journal of Nanomedicine & Biotherapeutic Discovery, 07(01). https://doi.org/10.4172/2155-983x.1000151

Murphy, C. J. (2002). MATERIALS science: NANOCUBES and Nanoboxes. Science, 298(5601), 2139–2141. https://doi.org/10.1126/science.1080007

Parveen, K., Banse, V., & Ledwani, L. (2016). Green synthesis of nanoparticles: Their advantages and disadvantages. https://doi.org/10.1063/1.4945168

Gour, A., & Jain, N. K. (2019). Advances in green synthesis of nanoparticles. Artificial Cells, Nanomedicine, and Biotechnology, 47(1), 844–851. https://doi.org/10.1080/21691401.2019.1577878

Brust, M., Walker, M., Bethell, D., Schiffrin, D. J., & Whyman, R. (1994). Synthesis of thiol-derivatised gold nanoparticles in a two-phase Liquid–Liquid system. J. Chem. Soc., Chem. Commun., (7), 801–802. https://doi.org/10.1039/c39940000801

Lee, K. X., Shameli, K., Yew, Y. P., Teow, S.-Y., Jahangirian, H., Rafiee-Moghaddam, R., & Webster, T. (2020). recent developments in the facile bio-synthesis of gold nanoparticles (aunps) and their biomedical applications. International Journal of Nanomedicine, Volume 15, 275–300. https://doi.org/10.2147/ijn.s233789

Hernández-Díaz, J. A., Garza-García, J. J. O., Zamudio-Ojeda, A., León-Morales, J. M., López-Velázquez, J. C., & García-Morales, S. (2020). Plant-mediated synthesis of nanoparticles and their antimicrobial activity against phytopathogens. Journal of the Science of Food and Agriculture, 101(4), 1270–1287. https://doi.org/10.1002/jsfa.10767

Iravani, S. (2011). Green synthesis of metal nanoparticles using plants. Green Chemistry, 13(10), 2638. https://doi.org/10.1039/c1gc15386b

Mittal, A. K., Chisti, Y., & Banerjee, U. C. (2013). Synthesis of metallic nanoparticles using plant extracts. Biotechnology Advances, 31(2), 346–356. https://doi.org/10.1016/j.biotechadv.2013.01.003

Nasrollahzadeh, M., Sajadi, S. M., Issaabadi, Z., & Sajjadi, M. (2019). Biological sources used in green nanotechnology. Interface Science and Technology, 81–111. https://doi.org/10.1016/b978-0-12-813586-0.00003-1

Gardea-Torresdey, J. L., Parsons, J. G., Gomez, E., Peralta-Videa, J., Troiani, H. E., Santiago, P., & Yacaman, M. J. (2002). Formation and growth of Au NANOPARTICLES inside LIVE Alfalfa Plants. Nano Letters, 2(4), 397–401. https://doi.org/10.1021/nl015673+

Naik, R. R., Stringer, S. J., Agarwal, G., Jones, S. E., & Stone, M. O. (2002). Biomimetic synthesis and patterning of silver nanoparticles. Nature Materials, 1(3), 169–172. https://doi.org/10.1038/nmat758

Dubey, S. P., Lahtinen, M., & Sillanpää, M. (2010). Tansy fruit mediated greener synthesis of silver and gold nanoparticles. Process Biochemistry, 45(7), 1065–1071. https://doi.org/10.1016/j.procbio.2010.03.024

Dwivedi, A. D., & Gopal, K. (2010). Biosynthesis of silver and gold nanoparticles using Chenopodium album leaf extract. Colloids and Surfaces A: Physicochemical and Engineering Aspects, 369(1-3), 27–33. https://doi.org/10.1016/j.colsurfa.2010.07.020

Armendariz, V., Herrera, I., peralta-videa, J. R., Jose-yacaman, M., Troiani, H., Santiago, P., & Gardea-Torresdey, J. L. (2004). Size controlled gold nanoparticle

formation by Avena sativa biomass: Use of plants in nanobiotechnology. Journal of Nanoparticle Research, 6(4), 377–382. https://doi.org/10.1007/s11051-004-0741-4

Costa, L. H., Hemmer, J. V., Wanderlind, E. H., Gerlach, O. M., Santos, A. L., Tamanaha, M. S., Bella-Cruz, A., Corrêa, R., Bazani, H. A., Radetski, C. M., & Almerindo, G. I. (2020). Green synthesis of gold nanoparticles obtained from algae Sargassum cymosum: Optimization, characterization and stability. BioNanoScience, 10(4), 1049–1062. https://doi.org/10.1007/s12668-020-00776-4

Sheny, D. S., Mathew, J., & Philip, D. (2011). Phytosynthesis of au, ag and au–ag bimetallic nanoparticles using aqueous extract and dried leaf of anacardium occidentale. Spectrochimica Acta Part A: Molecular and Biomolecular Spectroscopy, 79(1), 254–262. https://doi.org/10.1016/j.saa.2011.02.051

Eskandari-Nojedehi, M., Jafarizadeh-Malmiri, H., & Rahbar-Shahrouzi, J. (2018). Hydrothermal Green synthesis of gold nanoparticles using mushroom (agaricus bisporus) extract: Physico-chemical characteristics and antifungal activity studies. Green Processing and Synthesis, 7(1), 38–47. https://doi.org/10.1515/gps-2017-0004

Schauss, A. G., Wu, X., Prior, R. L., Ou, B., Huang, D., Owens, J., Agarwal, A., Jensen, G. S., Hart, A. N., & Shanbrom, E. (2006). Antioxidant capacity and other bioactivities of the freeze-dried Amazonian palm berry, Euterpe Oleraceae Mart. (ACAI). Journal of Agricultural and Food Chemistry, 54(22), 8604–8610. https://doi.org/10.1021/jf0609779

Gallori, S., Bilia, A. R., Bergonzi, M. C., Barbosa, W. L. R., & Vincieri,

F. F. (2004). Polyphenolic constituents of fruit pulp of Euterpe

oleracea Mar t. (Acai palm). Chromatographia, 59(11-12). https://doi.org/10.1365/s10337-004-0305-x

de Oliveira, M. do, & Schwartz, G. (2018). Açaí— euterpe oleracea. Exotic Fruits, 1–5. https://doi.org/10.1016/b978-0-12-803138-4.00002-2 Mertens-Talcott, S. U., Rios, J., Jilma-Stohlawetz, P., Pacheco-Palencia, L. A., Meibohm, B., Talcott, S. T., & Derendorf, H. (2008). Pharmacokinetics of anthocyanins and antioxidant effects after the consumption of anthocyanin-rich açai juice and pulp (Euterpe Oleracea Mart.) in

human healthy volunteers. Journal of Agricultural and Food Chemistry, 56(17), 7796–7802. https://doi.org/10.1021/jf8007037

Hangun-Balkir, Y., & McKenney, M. L. (2012). Determination of antioxidant activities of berries and resveratrol. Green Chemistry Letters and Reviews, 5(2), 147–153. https://doi.org/10.1080/17518253.2011.603756

Freitas, H. V., Dos Santos Filho, A. L., Rodrigues, S., Abreu, V. K., Narain, N., Lemos, T. D., Gomes, W. F., & Pereira, A. L. (2021). Synbiotic Açaí Juice (Euterpe oleracea) containing sucralose as noncaloric sweetener: Processing optimization, bioactive compounds, and acceptance during storage. Journal of Food Science, 86(3), 730–739. https://doi.org/10.1111/1750-3841.15617

BARLA, A., TOPCU, G., OKSUZ, S., TUMEN, G., & KINGSTON, D. (2007). Identification of cytotoxic sesquiterpenes from laurus nobilis L. *Food Chemistry*, *104*(4), 1478–1484. https://doi.org/10.1016/j.foodchem.2007.02.019

Sharma, A., Singh, J., & Kumar, S. (2012). Bay leaves. *Handbook of Herbs and Spices*, 73–85. https://doi.org/10.1533/9780857095671.73

Sayyah, M., Saroukhani, G., Peirovi, A., & Kamalinejad, M. (2003). Analgesic and anti-in?ammatory activity of the leaf Essential Oil Oflaurus Nobilis Linn. *Phytotherapy Research*, *17*(7), 733–736. https://doi.org/10.1002/ptr.1197

Patrakar, R., Mansuriya, M., & Patil, P. (2012). Phytochemical and pharmacological review on Laurus nobilis. International journal of pharmaceutical and chemical sciences, 1(2), 595-602.

De Matteis, V., Cascione, M., Rizzello, L., Manno, D. E., Di Guglielmo, C., & Rinaldi, R. (2021). Synergistic effect induced by gold nanoparticles with polyphenols shell during thermal therapy: Macrophage inflammatory response and cancer cell death assessment. *Cancers*, *13*(14), 3610. https://doi.org/10.3390/cancers13143610

Boulila, A., Hassen, I., Haouari, L., Mejri, F., Amor, I. B., Casabianca, H., & Hosni, K. (2015). Enzyme-assisted extraction of bioactive compounds from bay leaves (laurus nobilis L.). *Industrial Crops and Products*, *74*, 485–493. https://doi.org/10.1016/j.indcrop.2015.05.050

Dias, M. I., Barros, L., Dueñas, M., Alves, R. C., Oliveira, M. B., Santos-Buelga, C., & Ferreira, I. C. F. R. (2014). Nutritional and antioxidant contributions of Laurus nobilis L. leaves: Would be more suitable a wild or a cultivated sample? *Food Chemistry*, *156*, 339–346. https://doi.org/10.1016/j.foodchem.2014.01.122

Ertaş, M., & Hakkı Alma, M. (2010). Pyrolysis of laurel (laurus nobilis L.) extraction residues in a fixed-bed reactor: Characterization of bio-oil and bio-char. *Journal of Analytical and Applied Pyrolysis*, *88*(1), 22–29. https://doi.org/10.1016/j.jaap.2010.02.006

Philip, D. (2010). Green synthesis of gold and silver nanoparticles using Hibiscus Rosa sinensis. *Physica E: Low-Dimensional Systems and Nanostructures*, *42*(5), 1417–1424. https://doi.org/10.1016/j.physe.2009.11.081

Sridhar, V., Park, B.-W., & Sitti, M. (2018). Light-driven Janus Hollow mesoporous tio2-AU Microswimmers. *Advanced Functional Materials*, *28*(25), 1704902. https://doi.org/10.1002/adfm.201704902

Zhou, D., Li, Y. C., Xu, P., McCool, N. S., Li, L., Wang, W., & Mallouk, T. E. (2017). Visible-light controlled catalytic cu2o–au micromotors. *Nanoscale*, *9*(1), 75–78. https://doi.org/10.1039/c6nr08088j

Wu, Y., Lin, X., Wu, Z., Möhwald, H., & He, Q. (2014). Self-propelled polymer multilayer Janus capsules for effective drug delivery and light-triggered release. *ACS Applied Materials & Interfaces*, *6*(13), 10476–10481. https://doi.org/10.1021/am502458h

Zhang, Q., Dong, R., Wu, Y., Gao, W., He, Z., & Ren, B. (2017). Light-driven AU-wo3@c Janus micromotors for rapid photodegradation of dye pollutants. *ACS Applied Materials & Interfaces*, *9*(5), 4674–4683. https://doi.org/10.1021/acsami.6b12081

Wang, J., Xiong, Z., Zhan, X., Dai, B., Zheng, J., Liu, J., & Tang, J. (2017). A silicon nanowire as a spectrally tunable light-driven nanomotor. *Advanced Materials*, *29*(30), 1701451. https://doi.org/10.1002/adma.201701451 Ertaş, M., & Hakkı Alma, M. (2010). Pyrolysis of laurel (laurus nobilis L.) extraction residues in a fixed-bed reactor: Characterization of bio-oil and bio-char. *Journal of Analytical and Applied Pyrolysis*, *88*(1), 22–29. https://doi.org/10.1016/j.jaap.2010.02.006

Kalia, A. (2018). Nanotechnology in bioengineering: Transmogrifying plant biotechnology. In *Omics Technologies and Bio-engineering: Volume 2: Towards Improving Quality of Life*. Elsevier Inc. https://doi.org/10.1016/B978-0-12-815870-8.00012-7